Supporting Information

Continuous-Flow Hydrogenation of Nitroaromatics in Microreactor with Mesoporous Pd@SBA-15

Kejie Chai [1,2], Runqiu Shen [1,2], Tingting Qi [1,2], Jianli Chen [1,3], Weike Su [1,2,*] and An Su [4,*]

[1] National Engineering Research Center for Process Development of Active Pharmaceutical Ingredients, Collaborative Innovation Center of Yangtze River Delta Region Green Pharmaceuticals, Zhejiang University of Technology, Hangzhou 310014, China; 15757117001@163.com (K.C.); shenrunqiu@foxmail.com (R.S.); qi.tting@foxmail.com (T.Q.); 220163@jxnhu.edu.cn (J.C.)

[2] Key Laboratory of Pharmaceutical Engineering of Zhejiang Province, Zhejiang University of Technology, Hangzhou 310014, China

[3] College of New Materials Engineering, Jiaxing Nanhu University, Jiaxing 314000, China

[4] College of Chemical Engineering, Zhejiang University of Technology, Hangzhou 310014, China

* Correspondence: suweike@zjut.edu.cn(W.S.); ansu@zjut.edu.cn (A.S.)

Table S1. The content of Pd investigated by ICP-OES/MS.

Entry	ICP-OES	ICP-OES	ICP-MS
	Pristine Pd@SBA-15	Running 24 hours Pd@SBA-15	Running 24 hours Reaction solution
Pd	5.02±0.01%(w/w)	5.01±0.01%(w/w)	trace

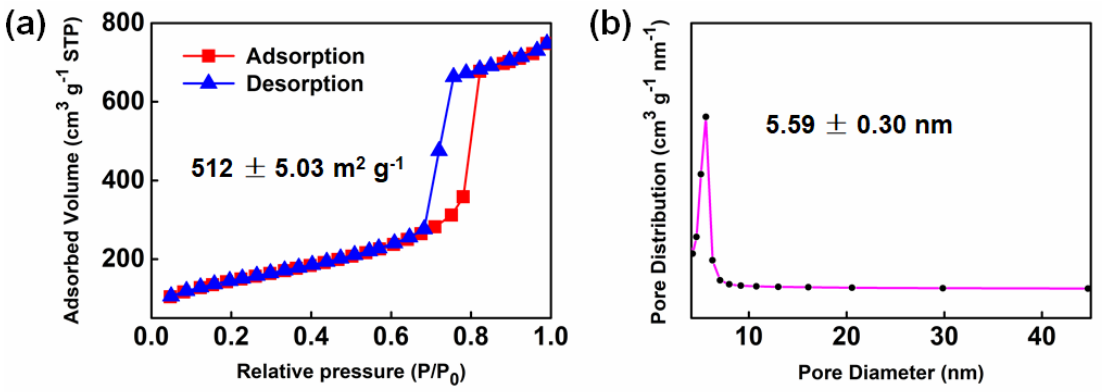

Figure S1. (a) N_2 adsorption-desorption isotherms and (b) pore size distribution of the SBA-15 treated similarly to the entire Pd@SBA-15 synthesis process without the addition of $PdCl_2$.

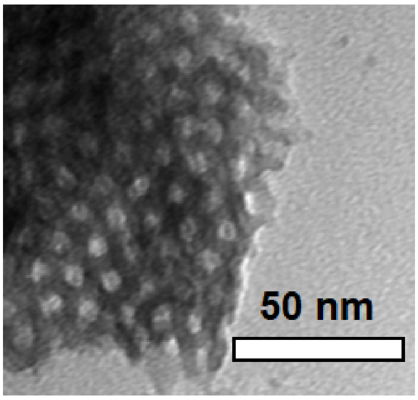

Figure S2. TEM image of Pd@SBA-15 after 24 h of reaction.

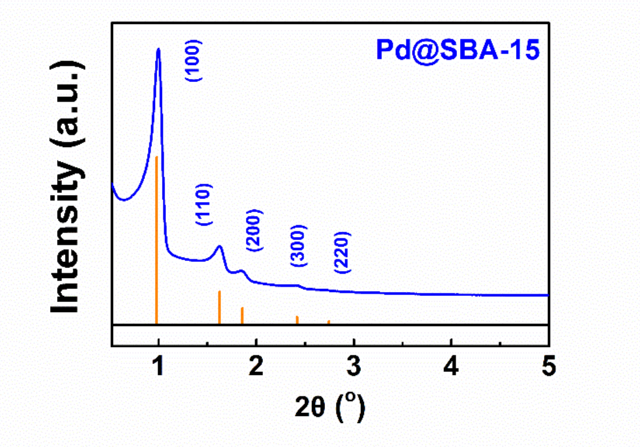

Figure S3. Small angle XRD pattern of Pd@SBA-15 after 24 h of reaction.

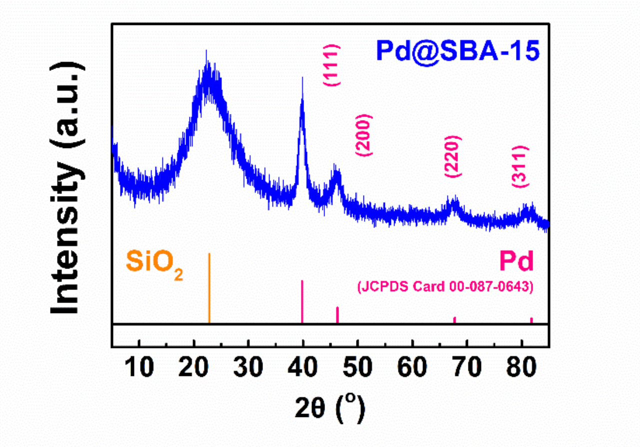

Figure S4. Wide-angle XRD pattern of Pd@SBA-15 after 24 h of reaction.

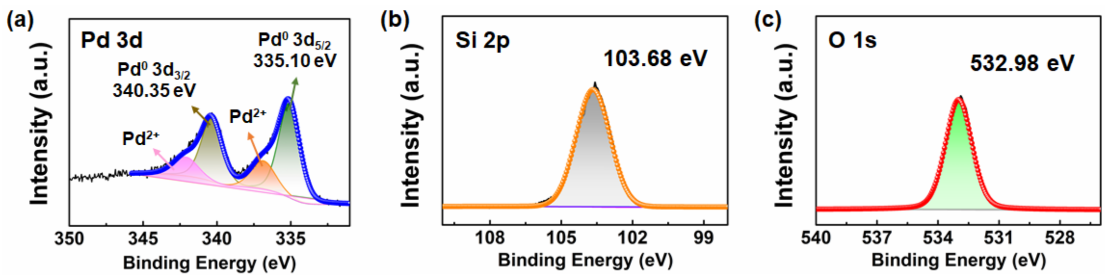

Figure S5. XPS spectrums of Pd@SBA-15 after 24 h of reaction: (a) Pd 3d, (b) Si 2p, (c) O 1s.

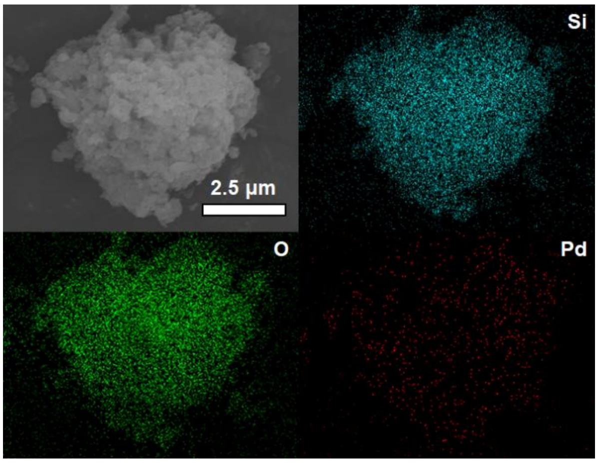

Figure S6. EDS elemental mappings of Pd@SBA-15 after 24 h of reaction.

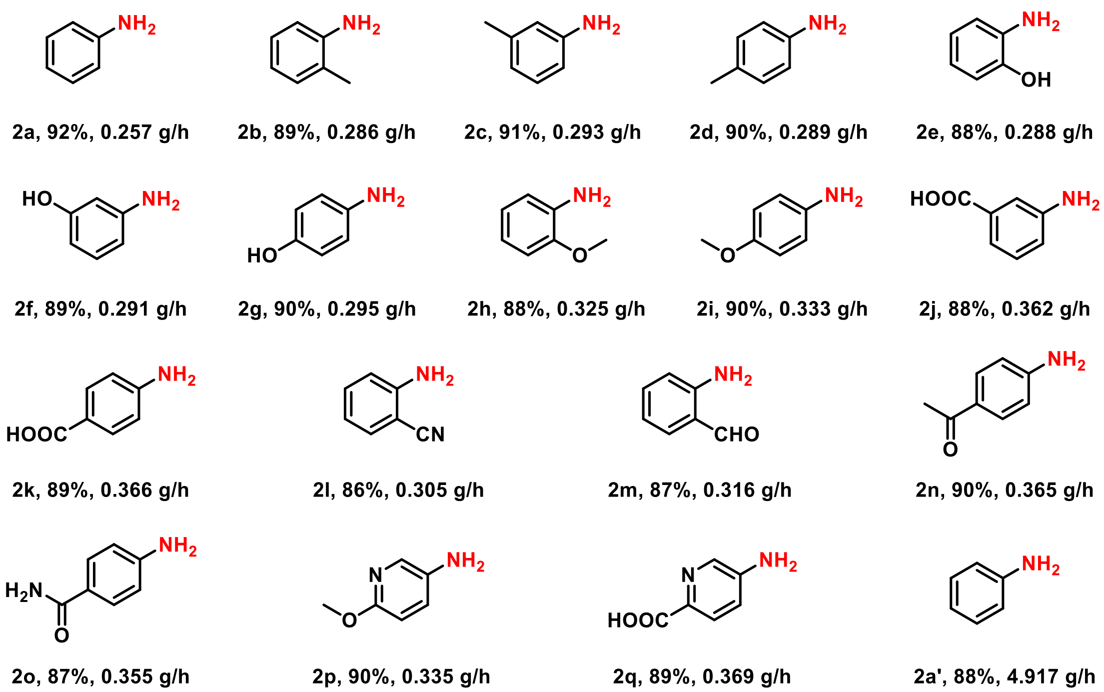

Scheme S1. Isolated yields and production rates of the obtained products.

Synthesis of SBA-15.

Mesoporous silica template SBA-15 was synthesized following the conventional method reported in the literature [1]. 6 g of Pluronic® P-123 and 30 mL of 12 M HCl were added to 195 g of water and the mixture was left to stand for 12 h to dissolve completely. 12.48 g TEOS was added to the above solution rapidly and stirred for 24 h at 38 ˚C and the white precipitation gradually appeared after about 15 min. The mixture was then transferred to a hydrothermal reactor with a polytetrafluoroethylene (PTFE) liner and hydrothermal treated at 120 ˚C for 24 h. After cooling the mixture to room temperature, it was filtered and washed thoroughly. The Pluronic® P-123 was then removed from the as-made sample by calcination in a muffle furnace at 550 ˚C in the air for 4 h (heating rate = 1.5 ˚C min^{-1}).

Characterization of the products

Aniline (2a) [2]

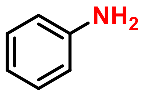

^{1}H NMR (500 MHz, $CDCl_3$) δ 7.18 – 7.11 (m, 2H), 6.78 – 6.72 (m, 1H), 6.69 – 6.63 (m, 2H), 3.57 (s, 2H).
^{13}C NMR (126 MHz, $CDCl_3$) δ 146.44 (s), 129.35 (s), 118.60 (s), 115.17 (s).

2-Toluidine (2b) [3]

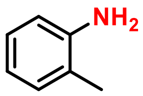

^{1}H NMR (500 MHz, $CDCl_3$) δ 7.02 (t, *J* = 7.9 Hz, 2H), 6.70 (t, *J* = 7.4 Hz, 1H), 6.65 (d, *J* = 7.8 Hz, 1H), 3.54 (s, 2H), 2.15 (s, 3H).
^{13}C NMR (126 MHz, $CDCl_3$) δ 144.59 (s), 130.50 (s), 127.02 (s), 122.39 (s), 118.69 (s), 115.00 (s), 17.40 (s).

3-Toluidine (2c) [3]

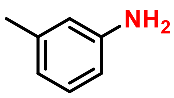

^{1}H NMR (500 MHz, DMSO) δ 6.88 (t, *J* = 7.6 Hz, 1H), 6.39 – 6.34 (m, 2H), 6.31 (d, *J* = 7.4 Hz, 1H), 4.88 (s, 2H), 2.14 (s, 3H).
^{13}C NMR (126 MHz, DMSO) δ 148.97 (s), 138.18 (s), 129.15 (s), 117.08 (s), 115.07 (s), 111.68 (s), 21.68 (s).

4-Toluidine (2d) [3]

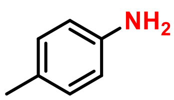

^{1}H NMR (500 MHz, DMSO) δ 6.81 (d, *J* = 8.1 Hz, 2H), 6.48 (d, *J* = 8.3 Hz, 2H), 4.75 (s, 2H), 2.12 (s, 3H).

^{13}C NMR (126 MHz, DMSO) δ 146.52 (s), 129.71 (s), 124.46 (s), 114.55 (s), 20.59 (s).

2-Aminophenol (2e) [2]

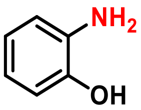

^{1}H NMR (500 MHz, DMSO) δ 8.90 (s, 1H), 6.62 (dd, *J* = 7.7, 1.3 Hz, 1H), 6.57 (dd, *J* = 7.7, 1.7 Hz, 1H), 6.52 (td, *J* = 7.5, 1.3 Hz, 1H), 6.38 (td, *J* = 7.5, 1.7 Hz, 1H), 4.44 (s, 2H).

^{13}C NMR (126 MHz, DMSO) δ 144.43 (s), 137.01 (s), 119.95 (s), 116.86 (s), 114.88 (s), 114.82 (s).

3-Aminophenol (2f) [4]

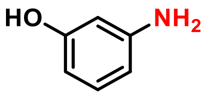

^{1}H NMR (500 MHz, DMSO) δ 8.82 (s, 1H), 7.01 – 6.55 (m, 1H), 6.00 (dd, *J* = 4.9, 2.7 Hz, 2H), 5.96 – 5.89 (m, 1H), 4.87 (s, 2H).

^{13}C NMR (126 MHz, DMSO) δ 158.52 (s), 150.26 (s), 129.88 (s), 105.89 (s), 103.77 (s), 101.43 (s).

4-Aminophenol (2g) [4]

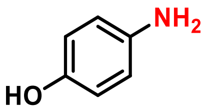

^{1}H NMR (500 MHz, DMSO) δ 8.35 (s, 1H), 6.51 – 6.46 (m, 2H), 6.45 – 6.40 (m, 2H), 4.36 (s, 2H).

^{13}C NMR (126 MHz, DMSO) δ 148.72 (s), 141.08 (s), 116.04 (s), 115.76 (s).

2-Anisidine (2h) [5]

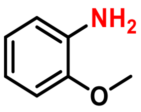

^{1}H NMR (500 MHz, DMSO) δ 6.77 (dd, *J* = 7.9, 0.8 Hz, 1H), 6.69 – 6.65 (m, 1H), 6.63 (dd, *J* = 7.7, 1.9 Hz, 1H), 6.52 (ddd, *J* = 7.9, 7.3, 1.9 Hz, 1H), 4.64 (s, 2H), 3.74 (s, 3H).

^{13}C NMR (126 MHz, DMSO) δ 146.82 (s), 138.05 (s), 121.32 (s), 116.65 (s), 114.29 (s), 111.01 (s), 55.64 (s).

4-Anisidine (2i) [5]

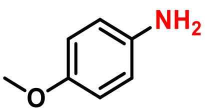

^{1}H NMR (500 MHz, $CDCl_3$) δ 6.76 – 6.68 (m, 2H), 6.65 – 6.56 (m, 2H), 3.72 (s, 3H), 3.41 (s, 2H).

^{13}C NMR (126 MHz, $CDCl_3$) δ 152.79 (s), 140.07 (s), 116.44 (s), 114.85 (s), 55.76 (s).

3-Aminobenzoic Acid (2j) [6]

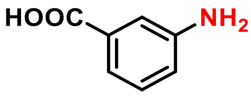

^{1}H NMR (500 MHz, DMSO) δ 12.51 (s, 1H), 7.22 – 7.17 (m, 1H), 7.15 – 7.06 (m, 2H), 6.80 – 6.75 (m, 1H), 5.34 (s, 2H).

^{13}C NMR (126 MHz, DMSO) δ 168.36 (s), 149.29 (s), 131.79 (s), 129.34 (s), 118.45 (s), 117.12 (s), 114.91 (s).

4-Aminobenzoic Acid (2k) [7]

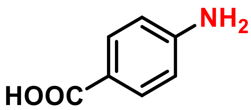

^{1}H NMR (500 MHz, DMSO) δ 11.93 (s, 1H), 7.70 – 7.49 (m, 2H), 6.64 – 6.42 (m, 2H), 5.86 (s, 2H).

^{13}C NMR (126 MHz, DMSO) δ 167.95 (s), 153.61 (s), 131.68 (s), 117.33 (s), 113.01 (s).

2-Aminobenzonitrile (2l) [8]

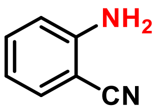

^{1}H NMR (500 MHz, DMSO) δ 7.38 (dd, *J* = 7.8, 1.4 Hz, 1H), 7.30 (ddd, *J* = 8.6, 7.3, 1.6 Hz, 1H), 6.84 – 6.77 (m, 1H), 6.64 – 6.54 (m, 1H), 6.02 (s, 2H).

^{13}C NMR (126 MHz, DMSO) δ 152.06 (s), 134.39 (s), 132.87 (s), 118.60 (s), 116.37 (s), 115.65 (s), 93.93 (s).

2-Aminobenzaldehyde (2m) [9]

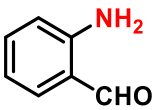

^{1}H NMR (500 MHz, DMSO) δ 9.82 (s, 1H), 7.53 (dd, *J* = 7.8, 1.5 Hz, 1H), 7.30 (ddd, *J* = 8.5, 7.1, 1.6 Hz, 1H), 7.12 (s, 2H), 6.77 (d, *J* = 8.4 Hz, 1H), 6.69 – 6.59 (m, 1H).

^{13}C NMR (126 MHz, DMSO) δ 194.45 (s), 151.15 (s), 136.04 (s), 135.52 (s), 118.23 (s), 116.29 (s), 115.40 (s).

4'-Aminoacetophenone (2n) [10]

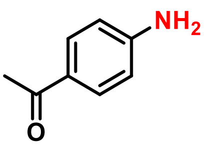

^{1}H NMR (500 MHz, $CDCl_3$) δ 7.79 – 7.65 (m, 2H), 6.67 – 6.43 (m, 2H), 4.13 (s, 2H), 2.42 (s, 3H).

^{13}C NMR (126 MHz, $CDCl_3$) δ 196.56 (s), 151.26 (s), 130.82 (s), 127.78 (s), 113.72 (s), 26.10 (s).

4-Aminobenzamide (2o) [11]

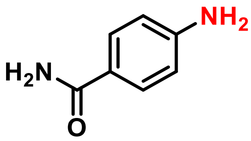

^{1}H NMR (500 MHz, DMSO) δ 7.62 – 7.56 (m, 2H), 7.52 (s, 1H), 6.84 (s, 1H), 6.57 – 6.47 (m, 2H), 5.59 (s, 2H).

^{13}C NMR (126 MHz, DMSO) δ 168.53 (s), 152.12 (s), 129.58 (s), 121.42 (s), 112.93 (s).

2-Methoxy-5-amino pyridine (2p) [12]

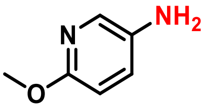

^{1}H NMR (500 MHz, $CDCl_3$) δ 7.66 (d, *J* = 2.8 Hz, 1H), 7.03 (dd, *J* = 8.7, 2.9 Hz, 1H), 6.60 (d, *J* = 8.7 Hz, 1H), 3.86 (s, 3H), 3.27 (s, 2H).

^{13}C NMR (126 MHz, $CDCl_3$) δ 158.08 (s), 136.65 (s), 132.86 (s), 127.65 (s), 110.72 (s), 53.33 (s).

5-Amino-2-pyridinecarboxylic acid (2q) [13]

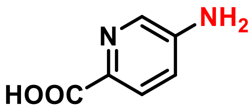

^{1}H NMR (500 MHz, DMSO) δ 11.56 (s, 1H), 7.95 (d, *J* = 19.0 Hz, 1H), 7.72 (dd, *J* = 21.1, 8.4 Hz, 1H), 7.02 – 6.78 (m, 1H), 6.11 (s, 2H).

^{13}C NMR (126 MHz, DMSO) δ 166.64 (s), 148.53 (s), 135.73 (s), 135.14 (s), 126.64 (s), 118.93 (s).

Aniline (2a’) [2]

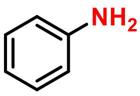

^{1}H NMR (600 MHz, DMSO) δ 7.03 (t, *J* = 7.8 Hz, 2H), 6.59 (d, *J* = 7.6 Hz, 2H), 6.51 (t, *J* = 7.3 Hz, 1H), 4.99 (s, 2H).

^{13}C NMR (151 MHz, DMSO) δ 149.05 (s), 129.28 (s), 116.19 (s), 114.41 (s).

Copies of ^{1}H and ^{13}C NMR Spectra

2a ^{1}H NMR

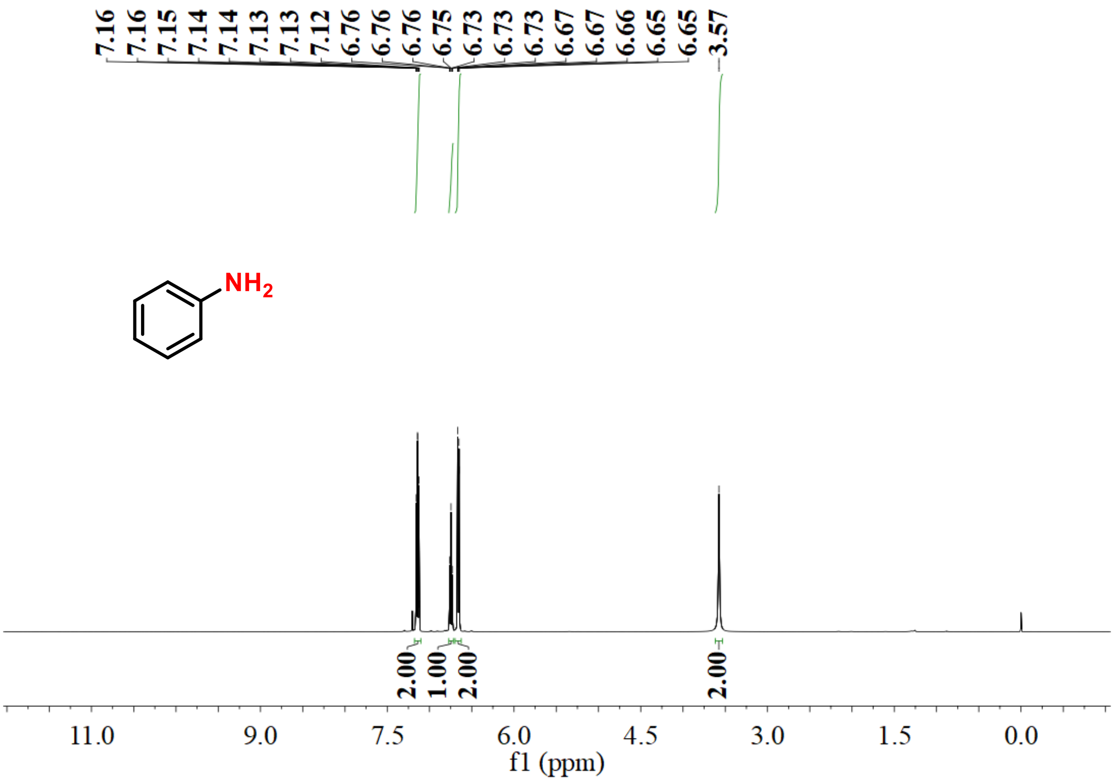

2a ^{13}C NMR

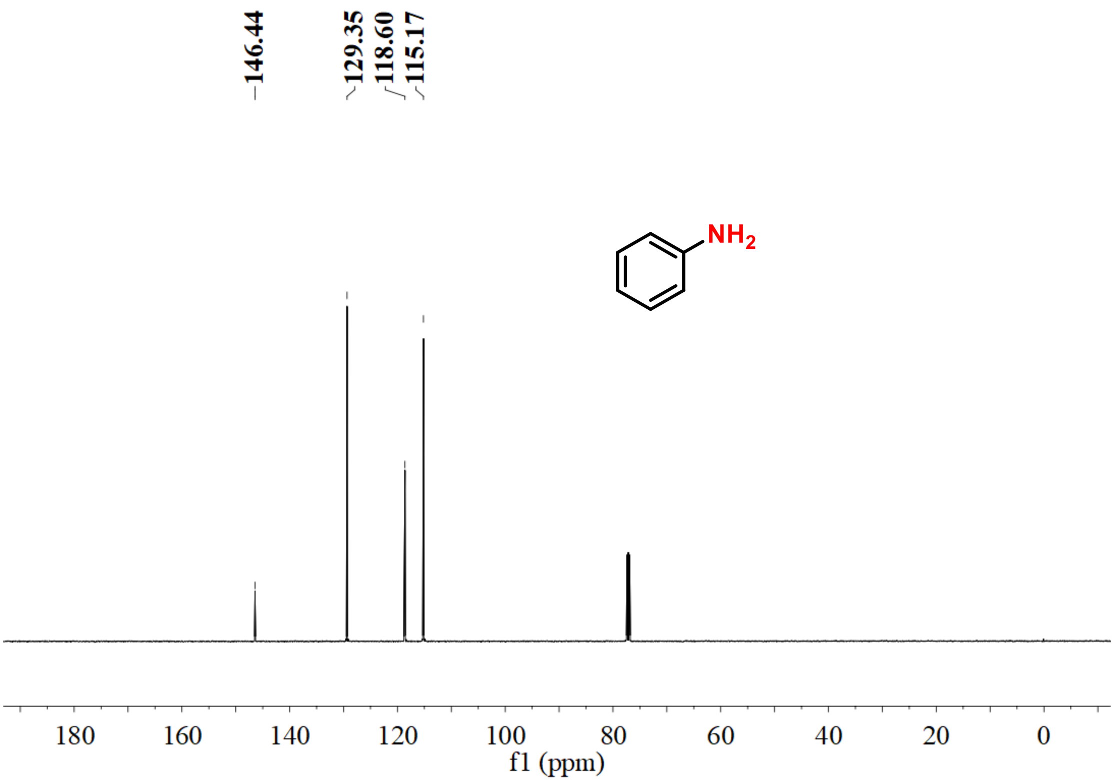

2b ^{1}H NMR

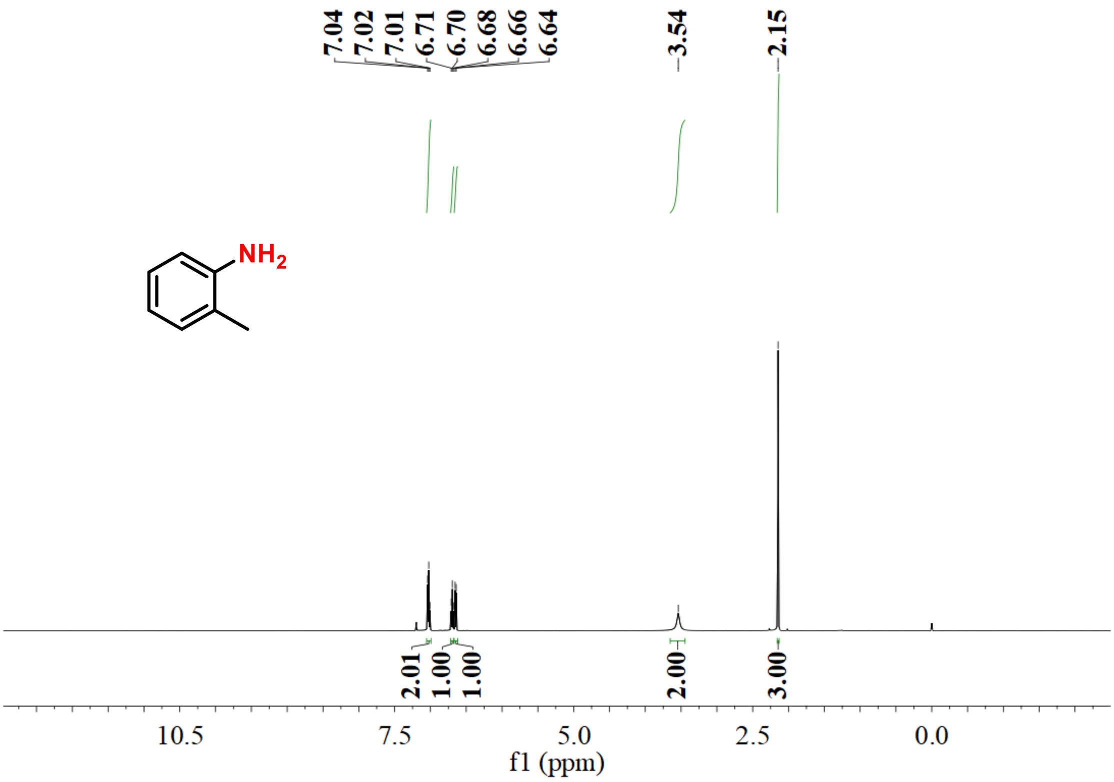

2b ^{13}C NMR

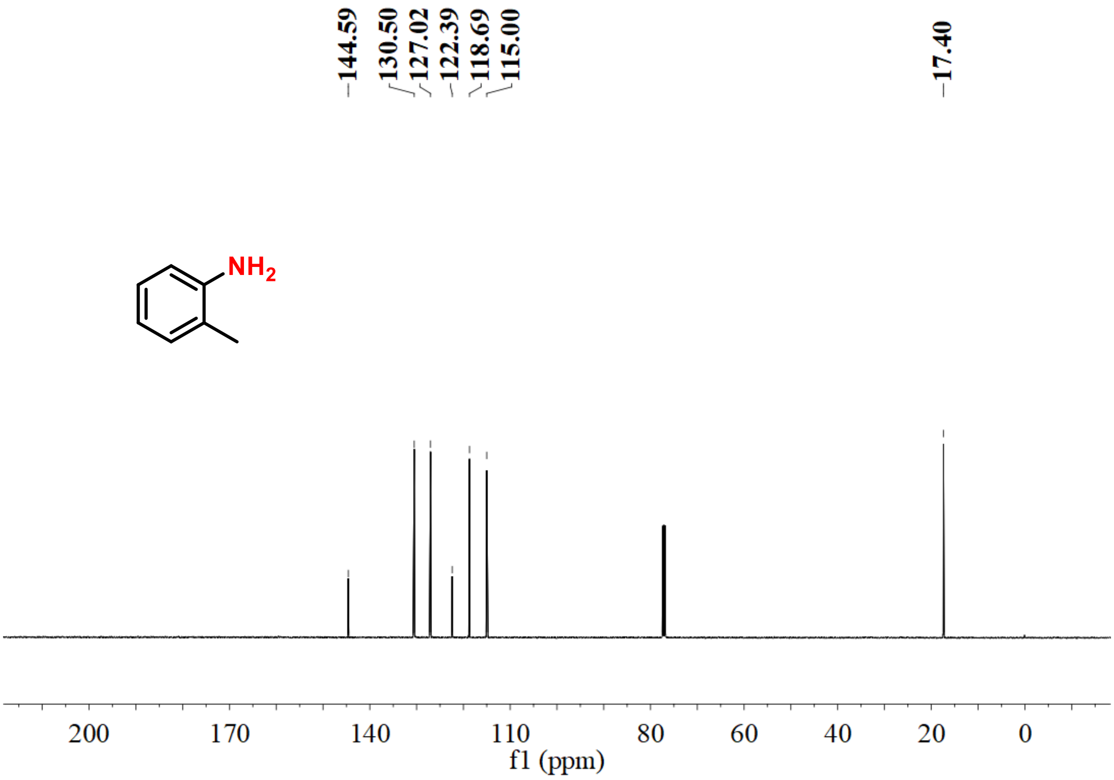

2c ^{1}H NMR

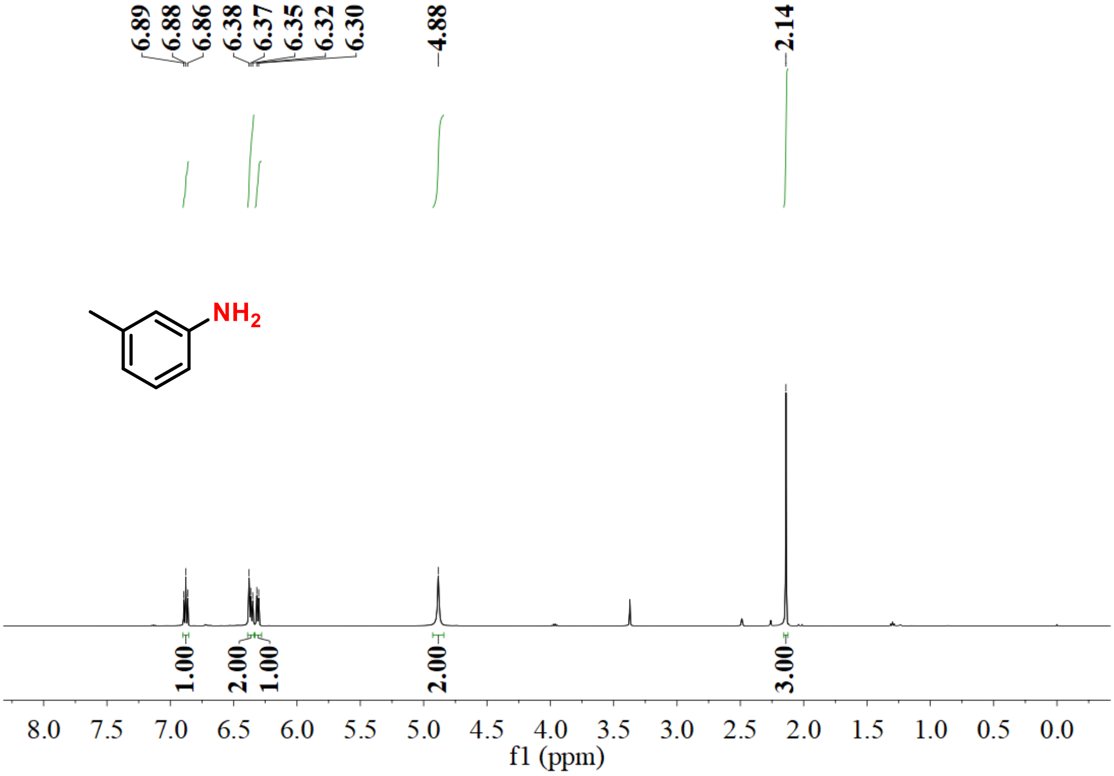

2c ^{13}C NMR

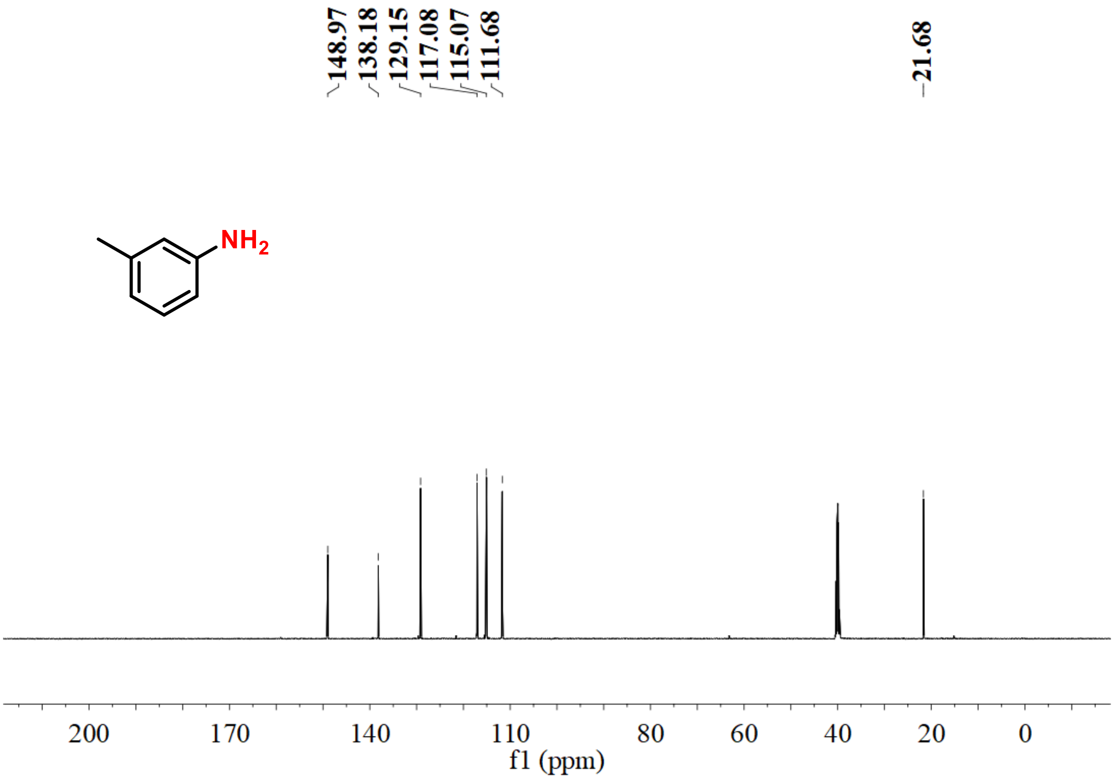

2d ¹H NMR

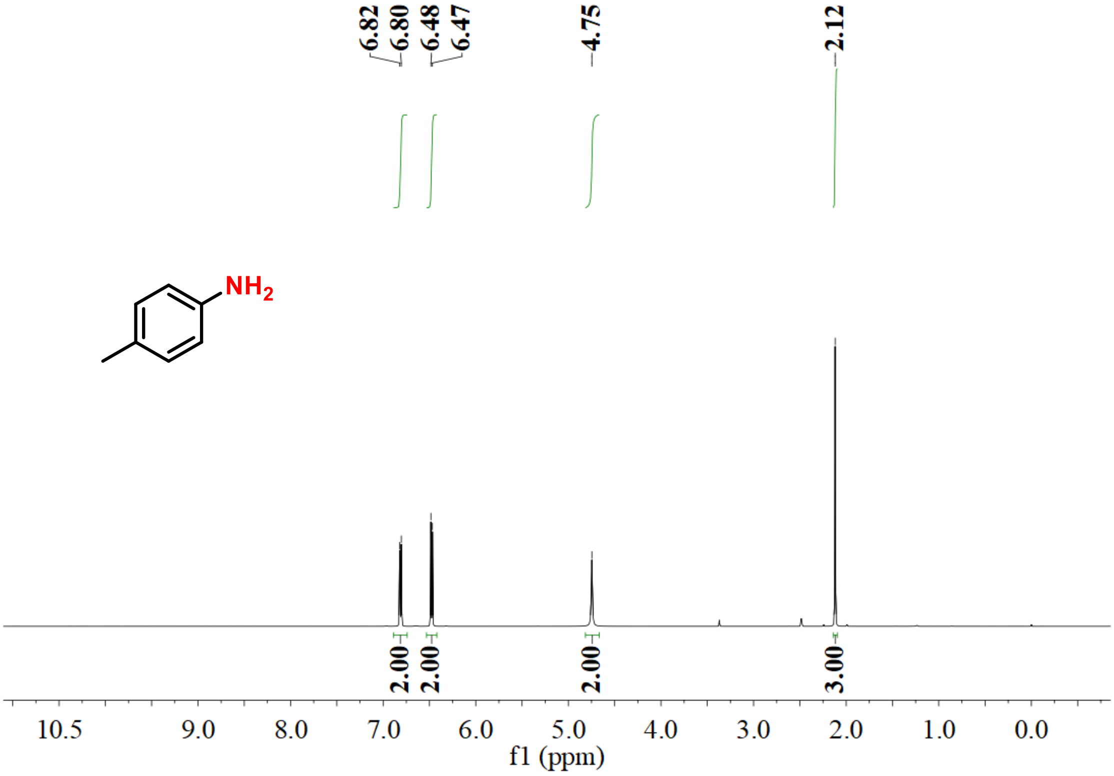

2d ¹³C NMR

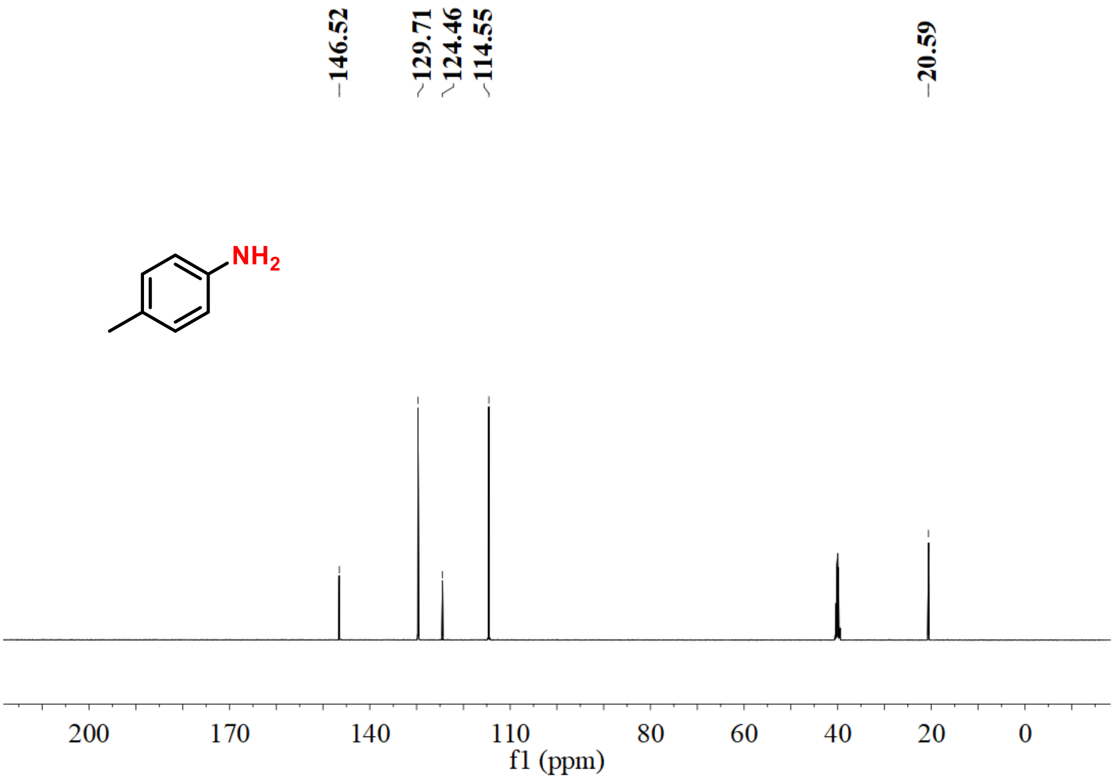

2e ^{1}H NMR

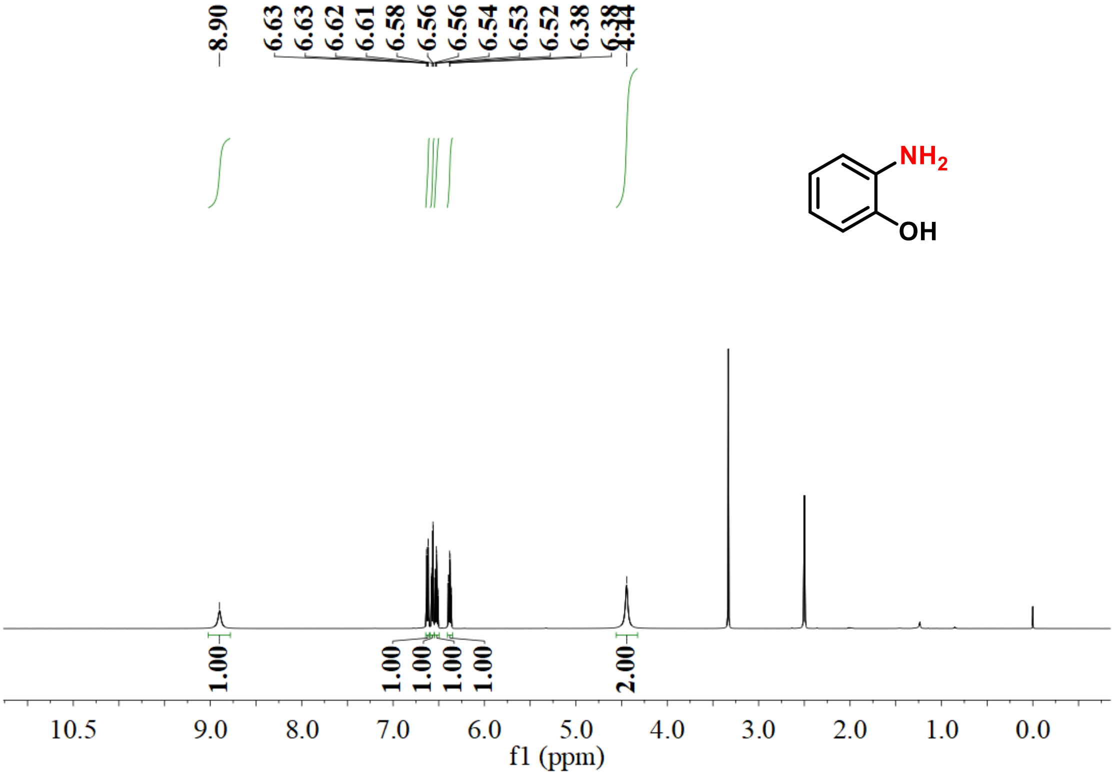

2e ^{13}C NMR

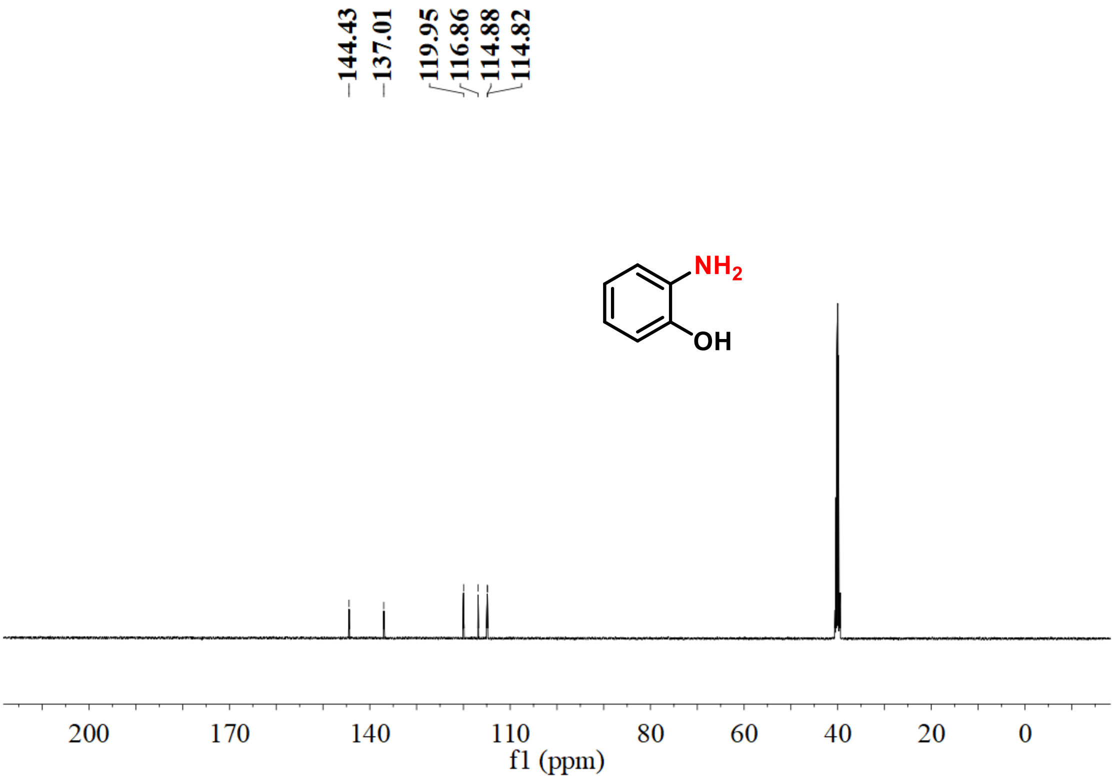

2f ^{1}H NMR

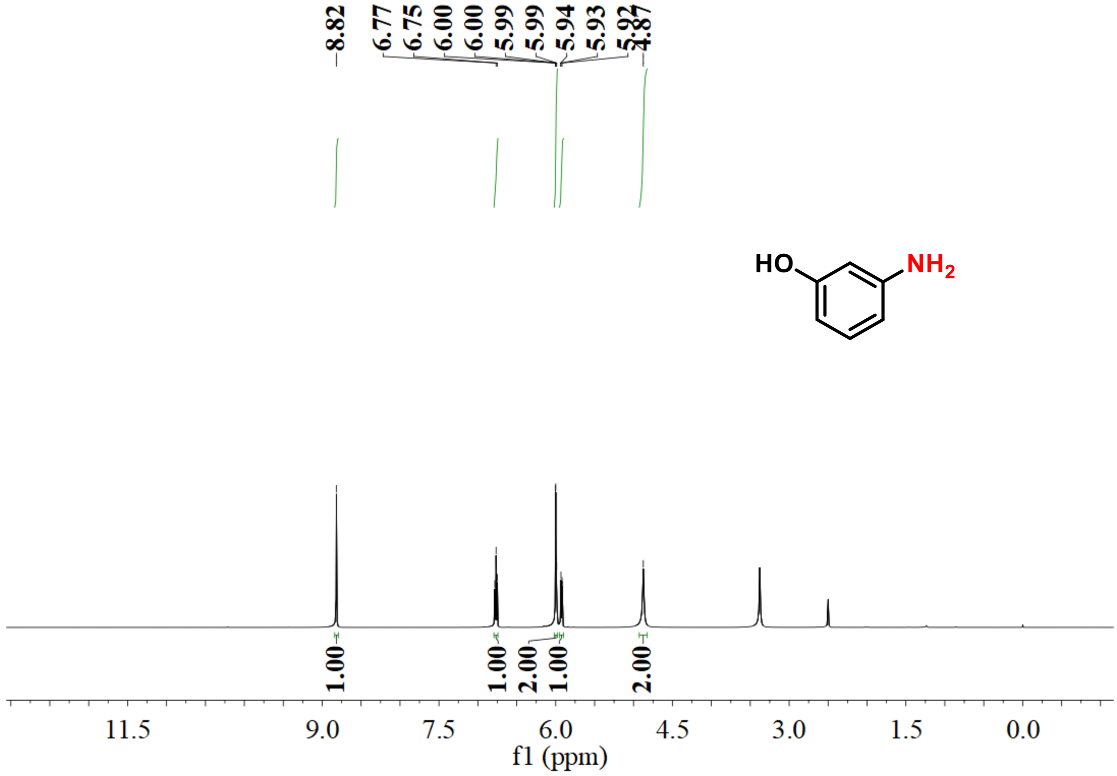

2f ^{13}C NMR

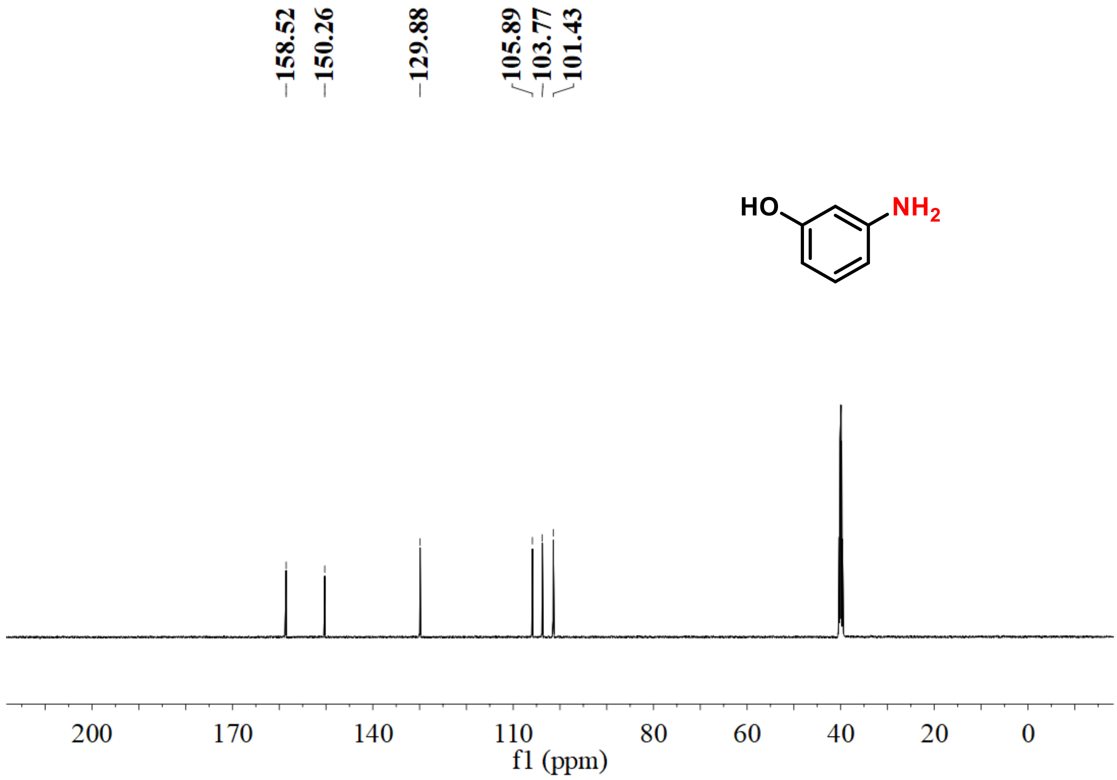

2g ^{1}H NMR

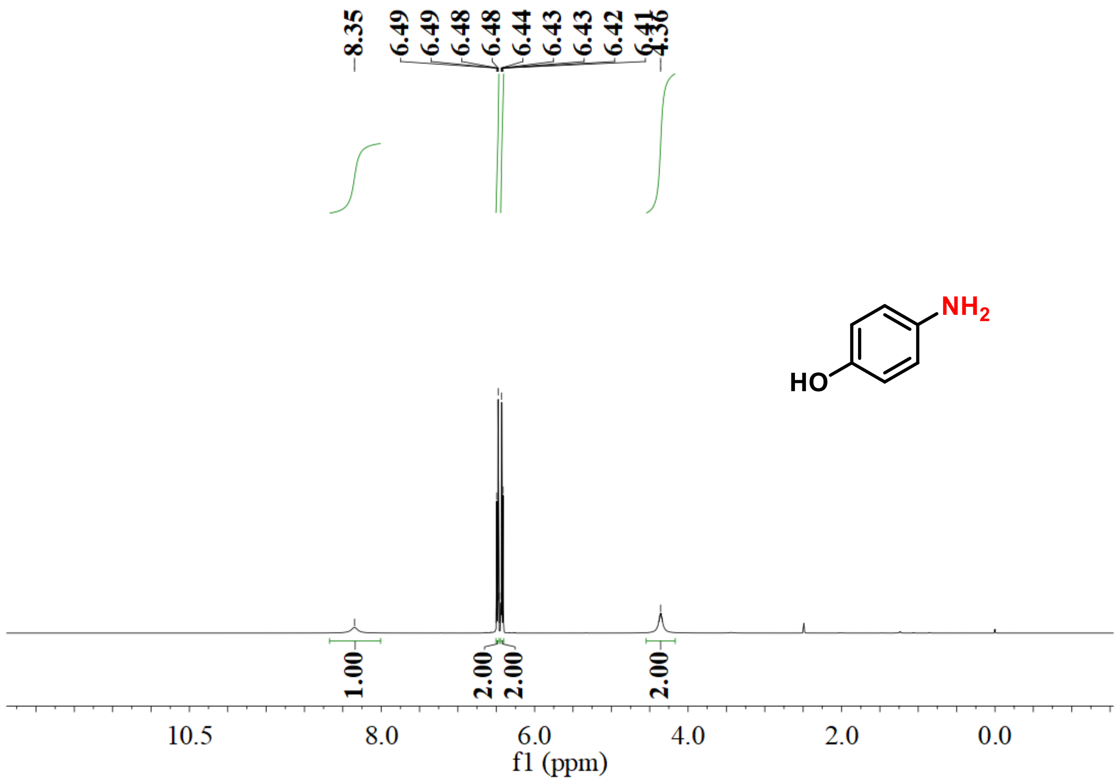

2g ^{13}C NMR

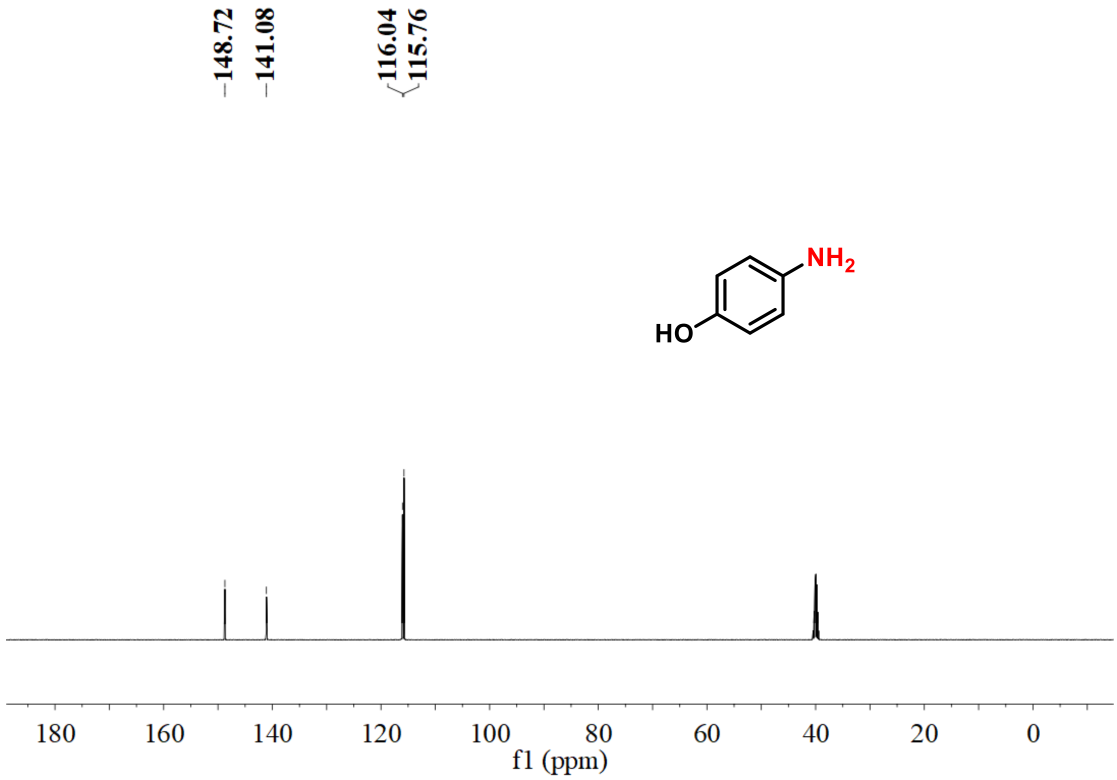

2h ¹H NMR

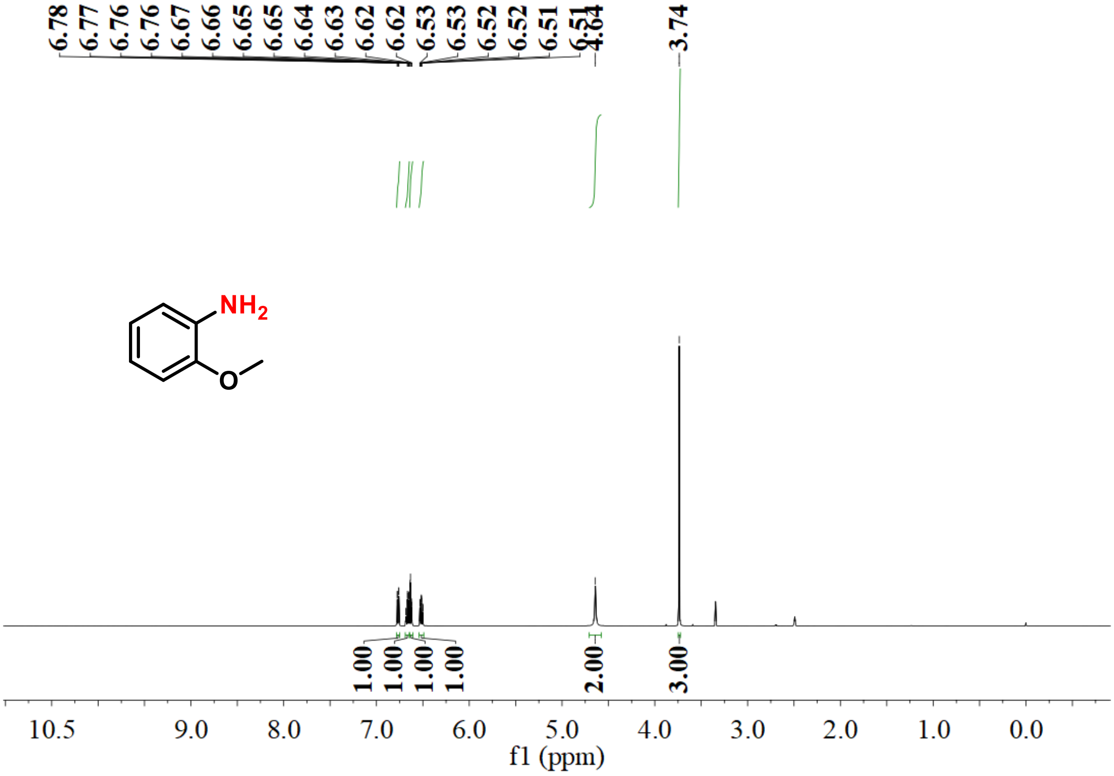

2h ¹³C NMR

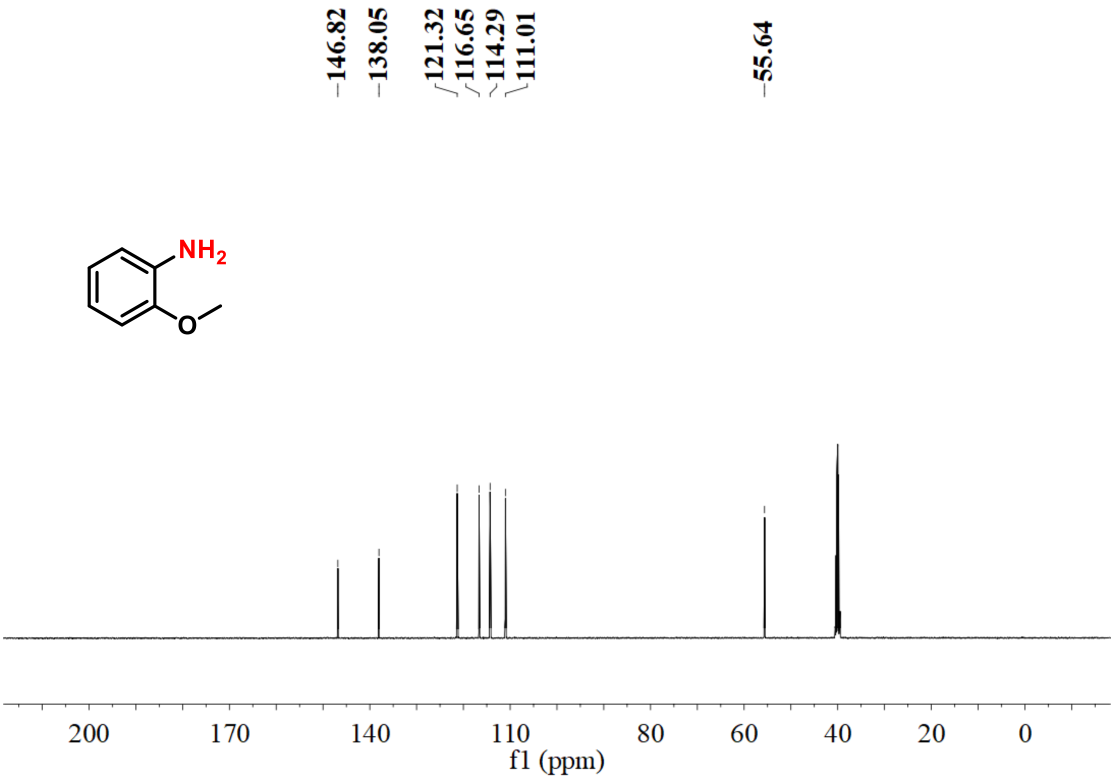

2i ^{1}H NMR

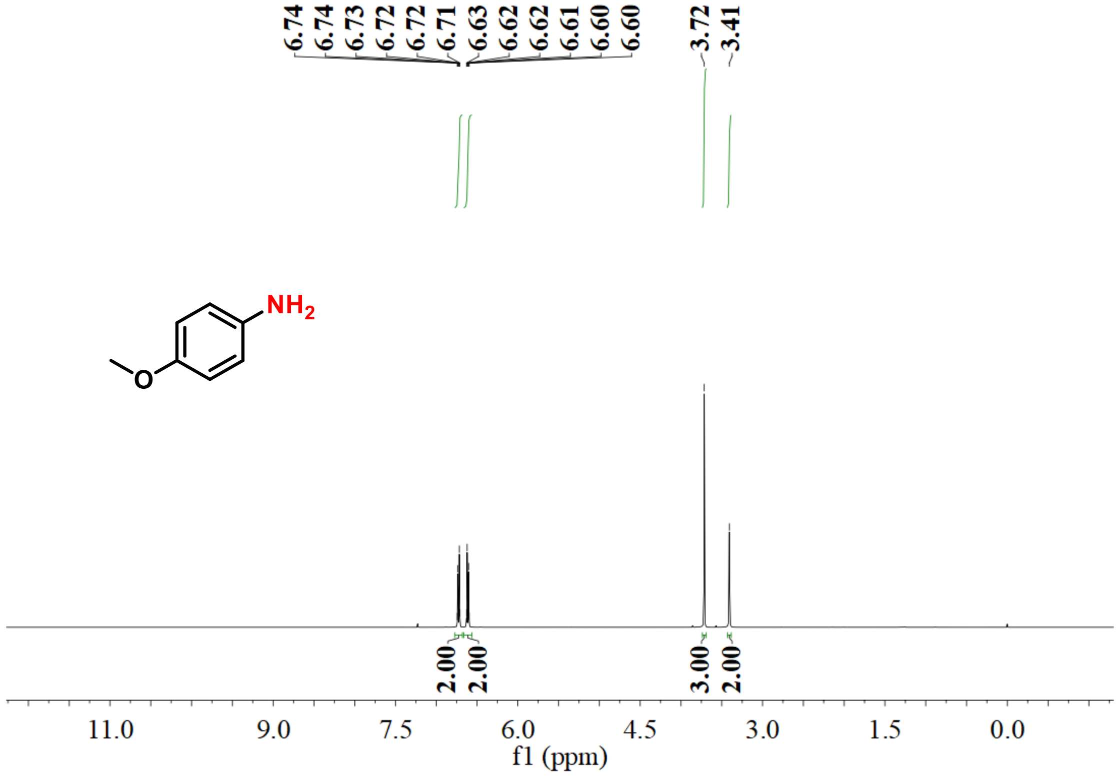

2i ^{13}C NMR

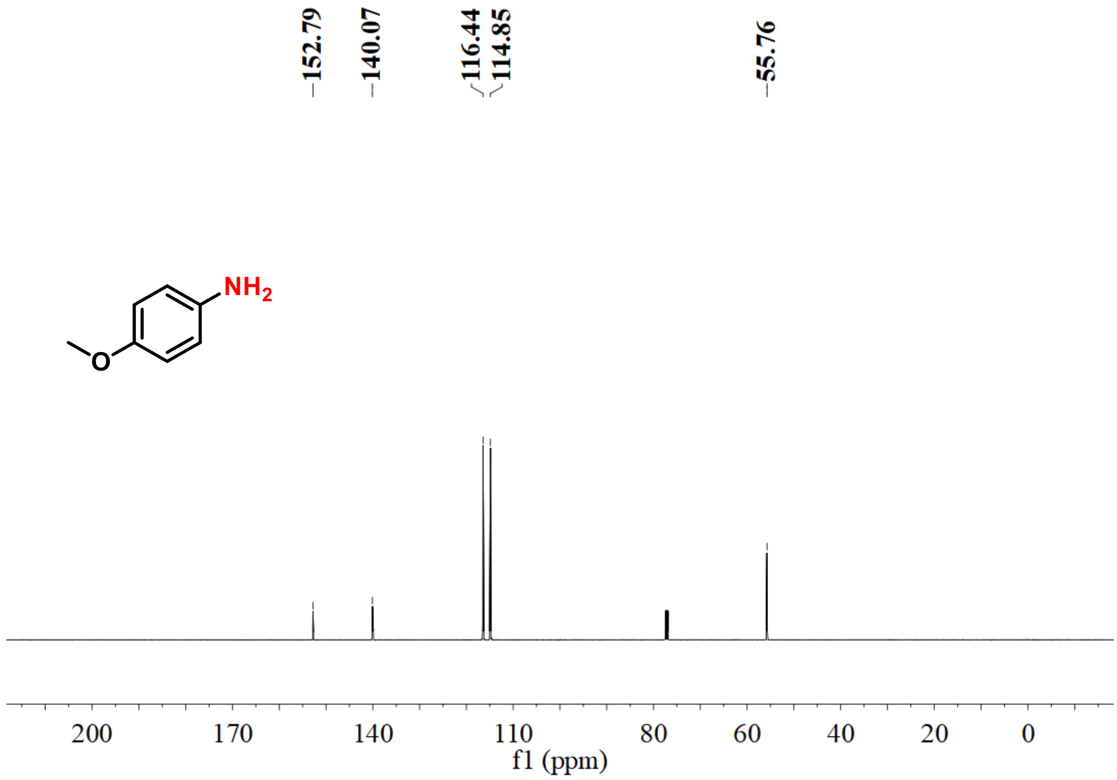

2j ^{1}H NMR

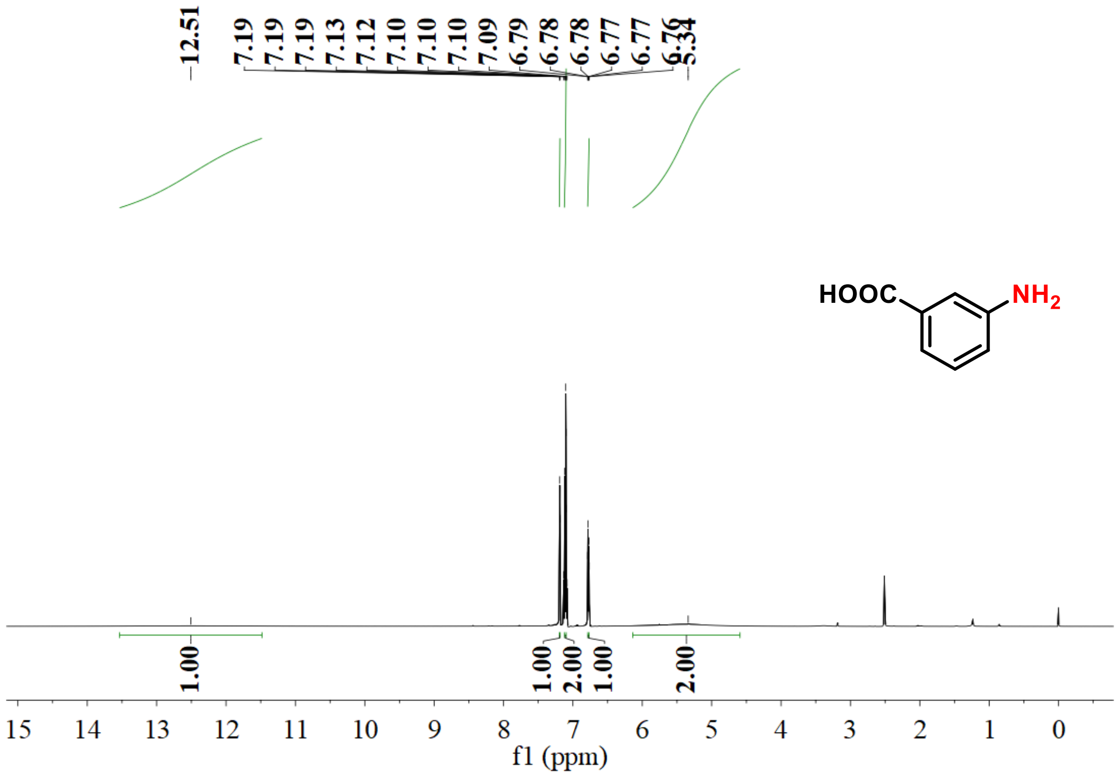

2j ^{13}C NMR

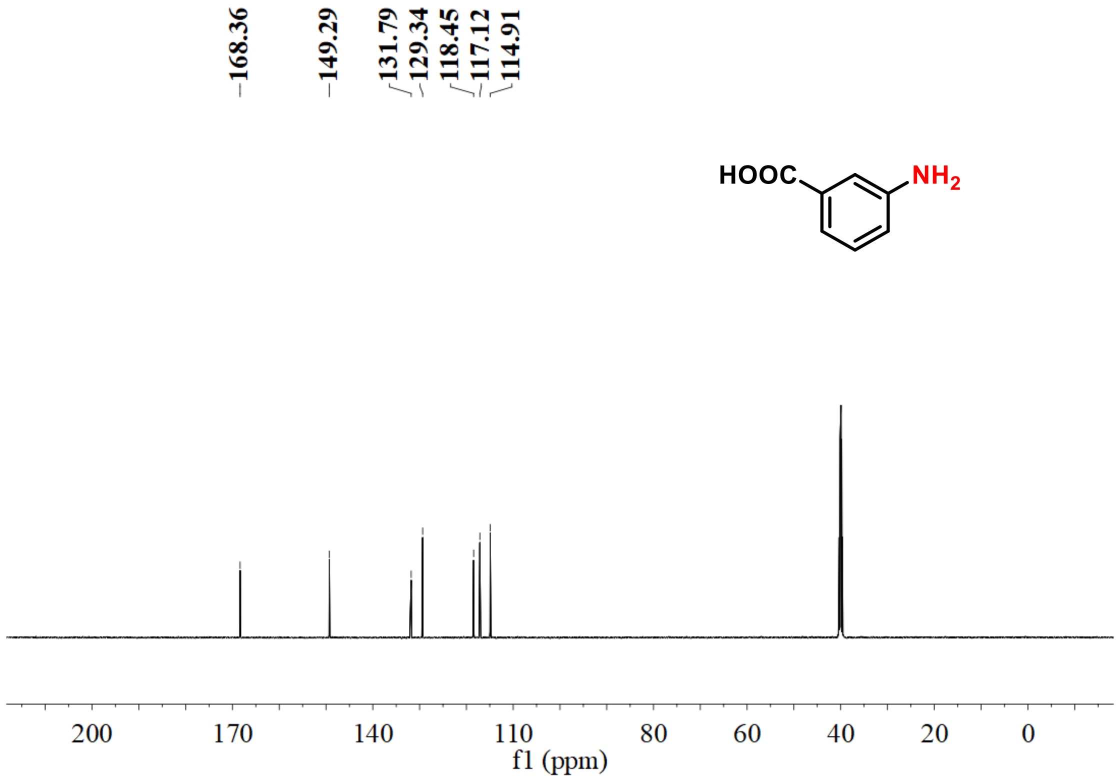

2k ¹H NMR

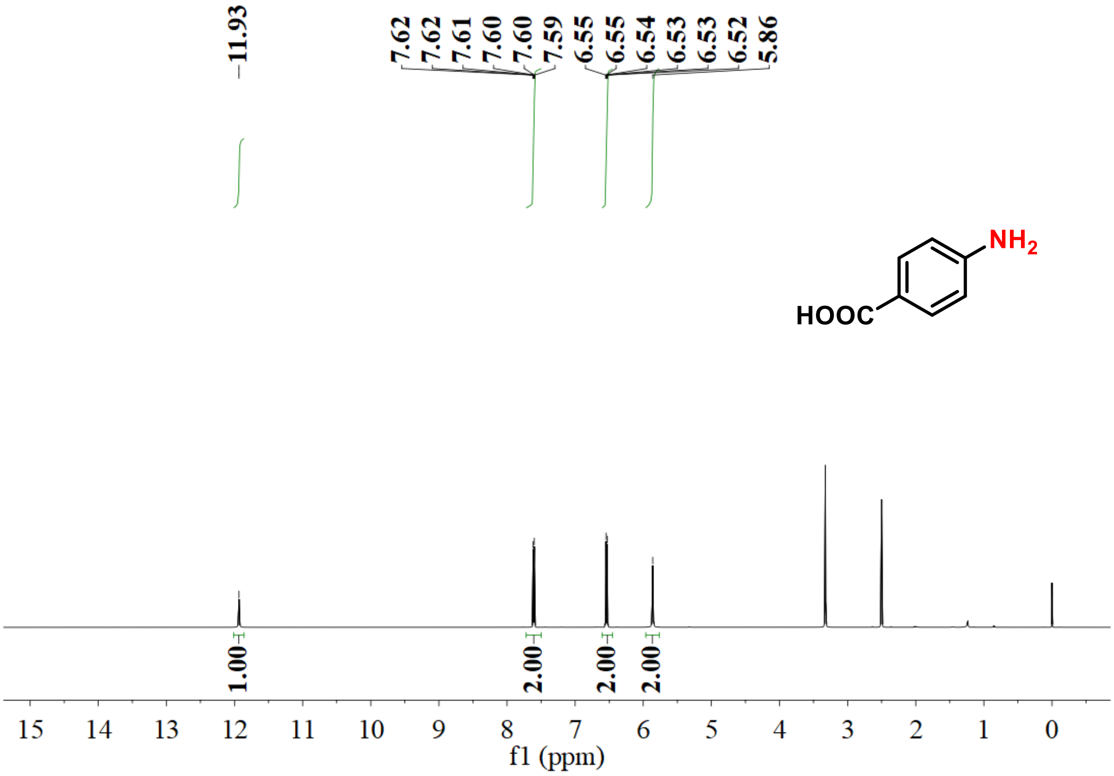

2k ¹³C NMR

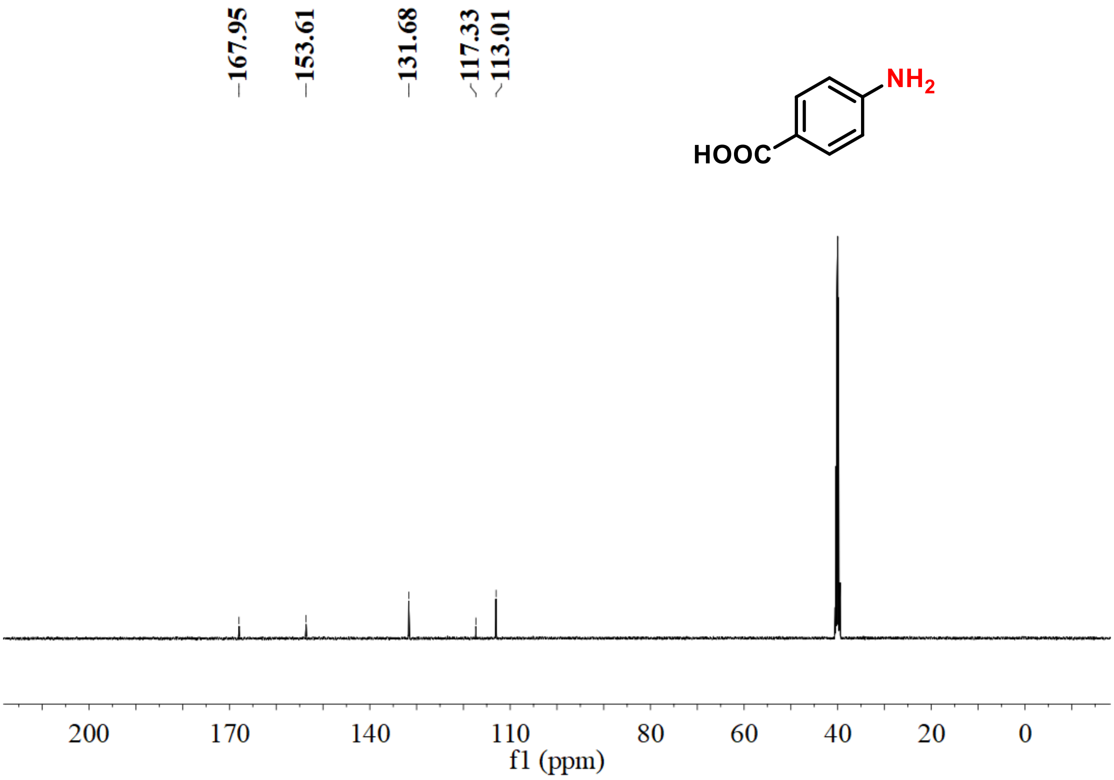

2l ¹H NMR

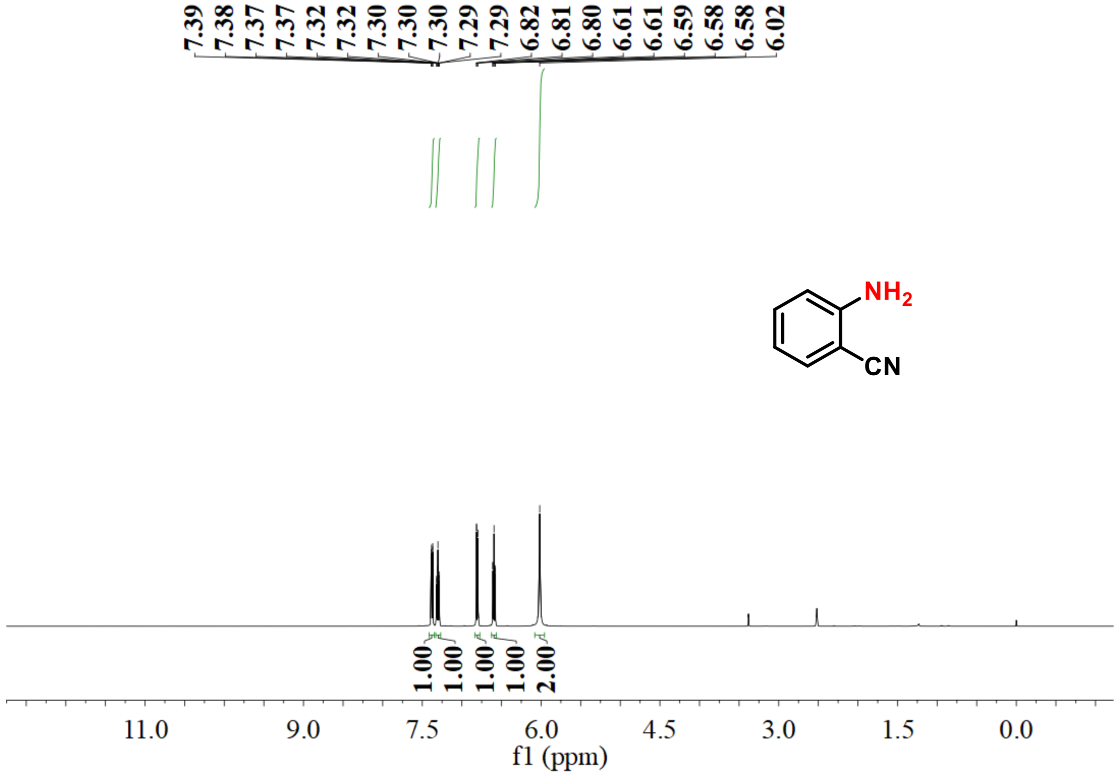

2l ¹³C NMR

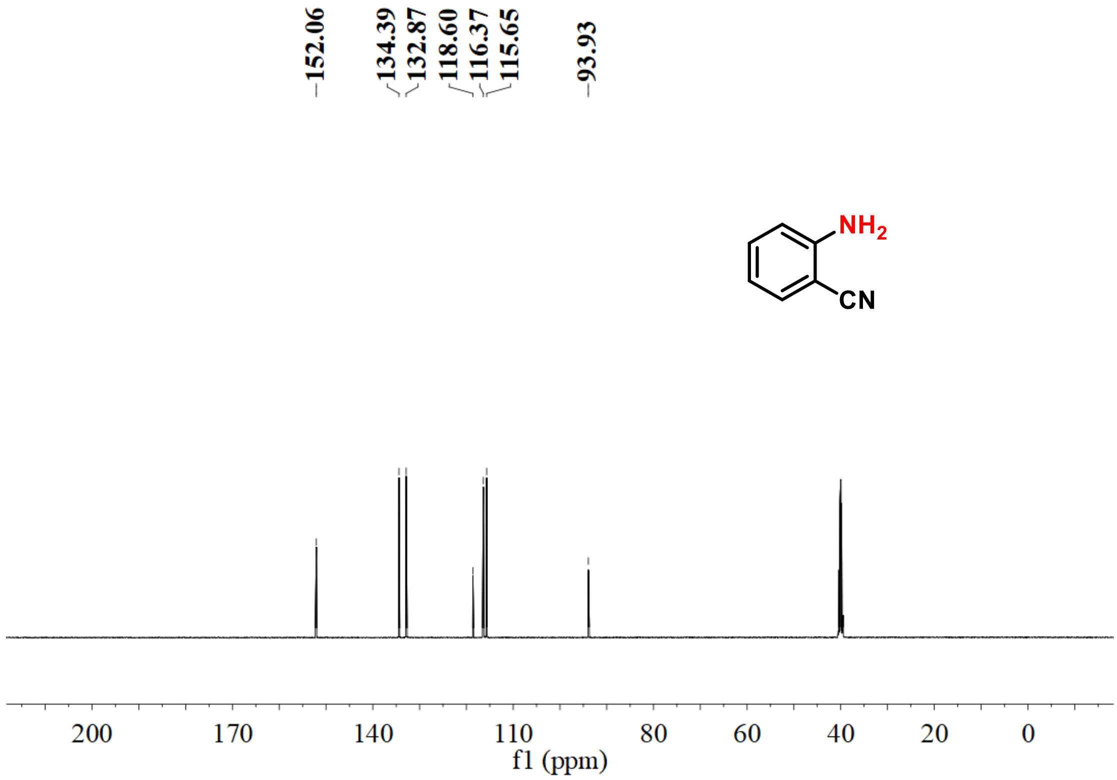

2m ^{1}H NMR

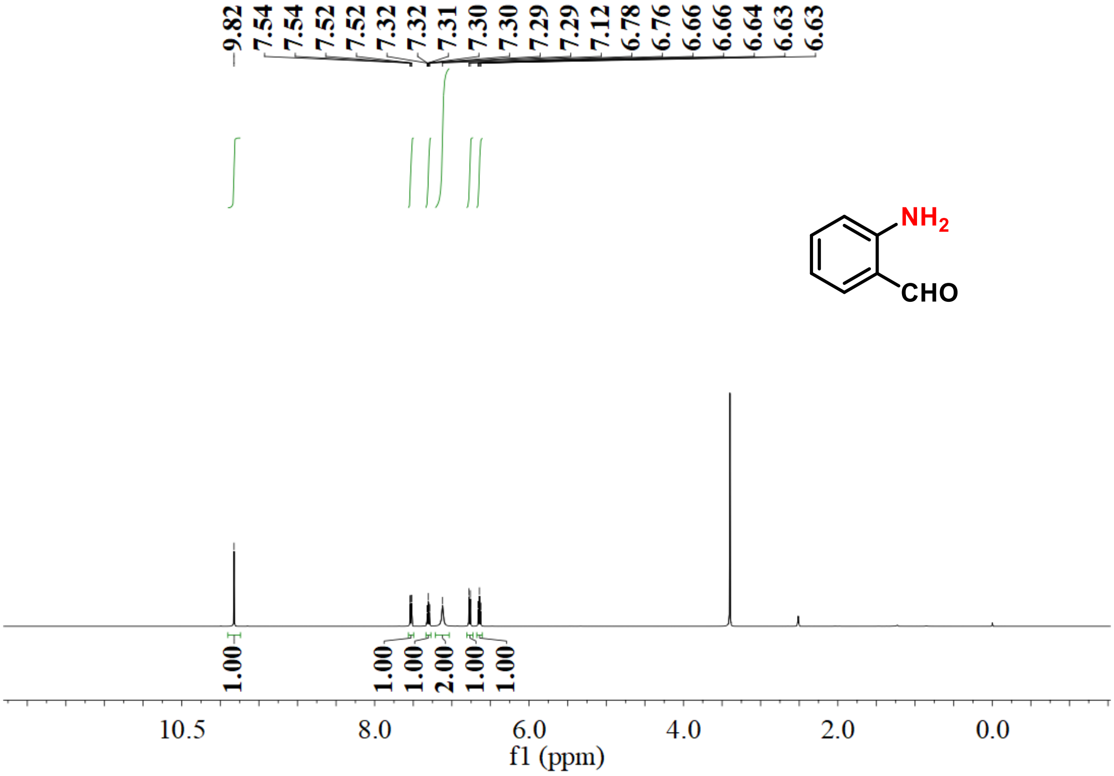

2m ^{13}C NMR

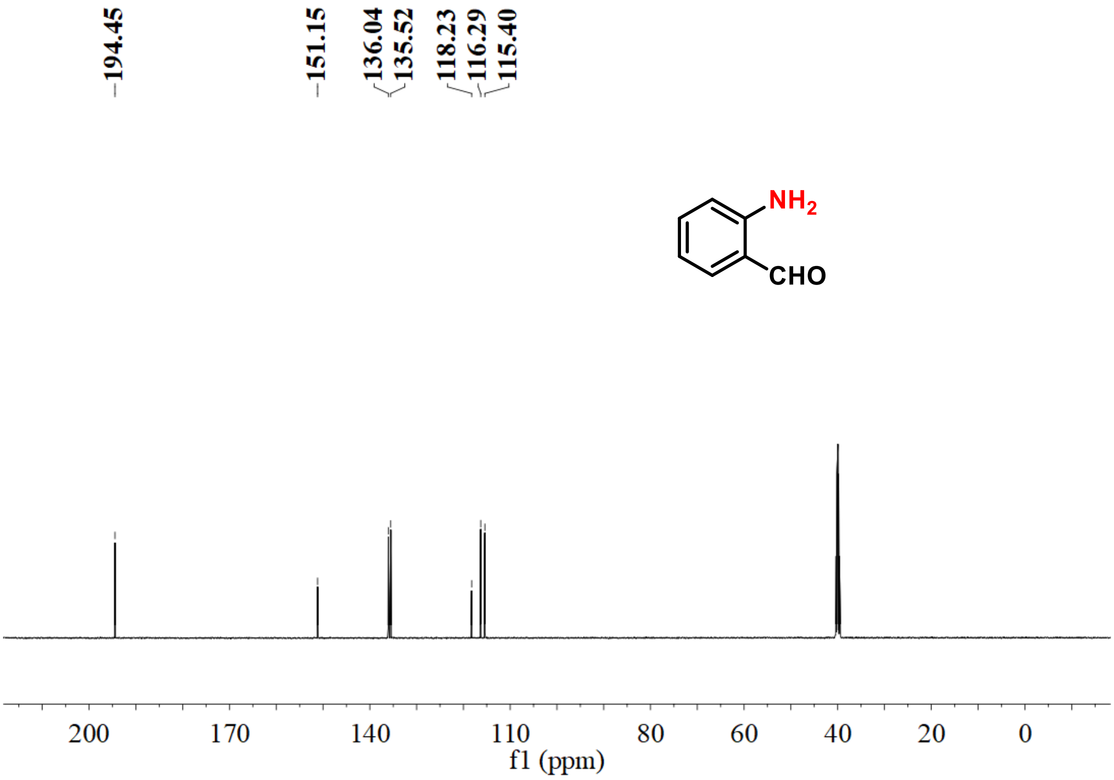

2n ^{1}H NMR

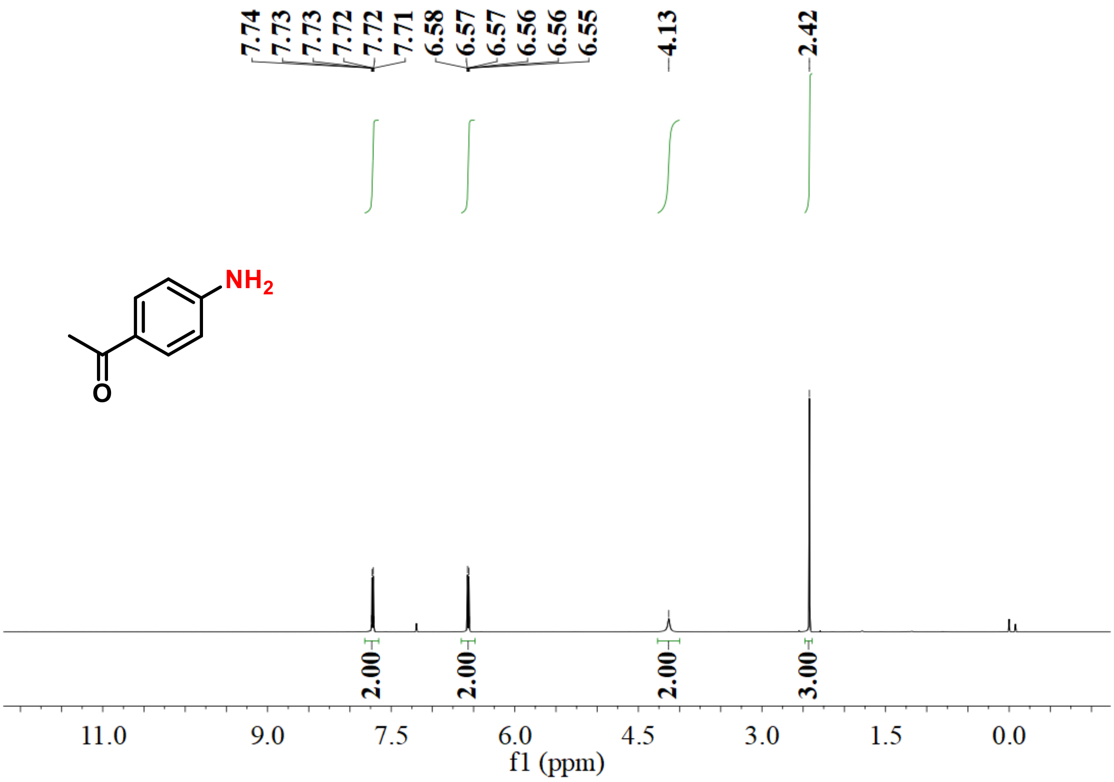

2n ^{13}C NMR

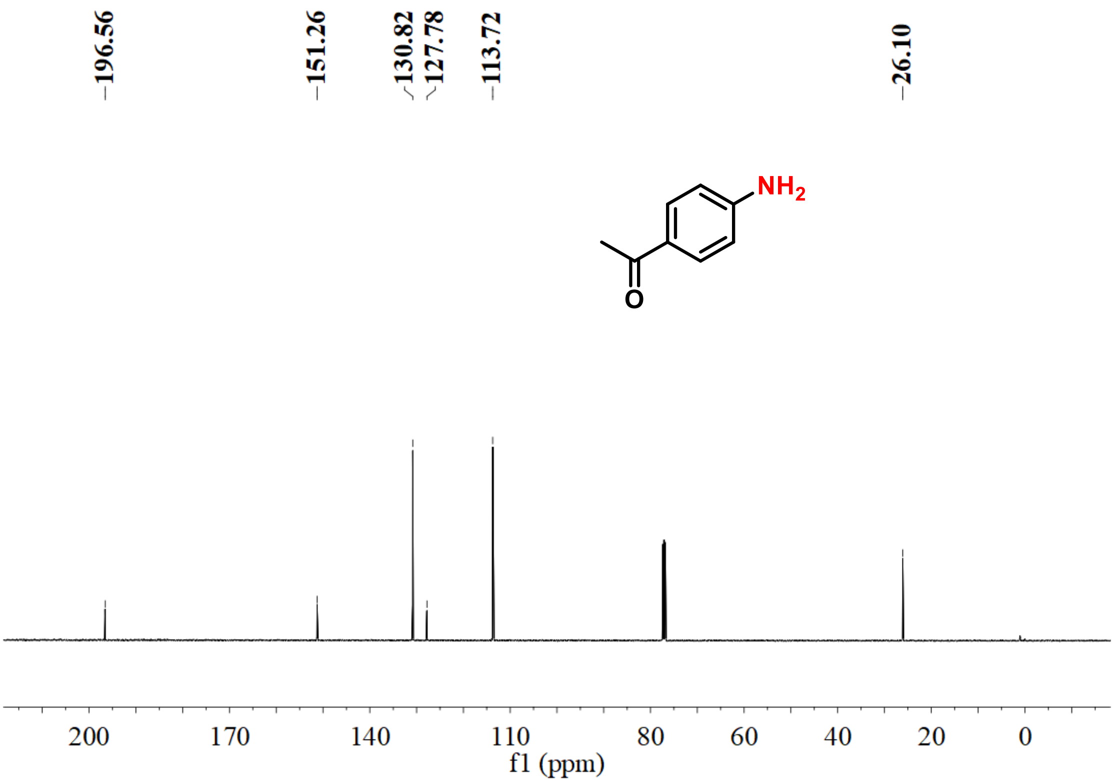

2o ^{1}H NMR

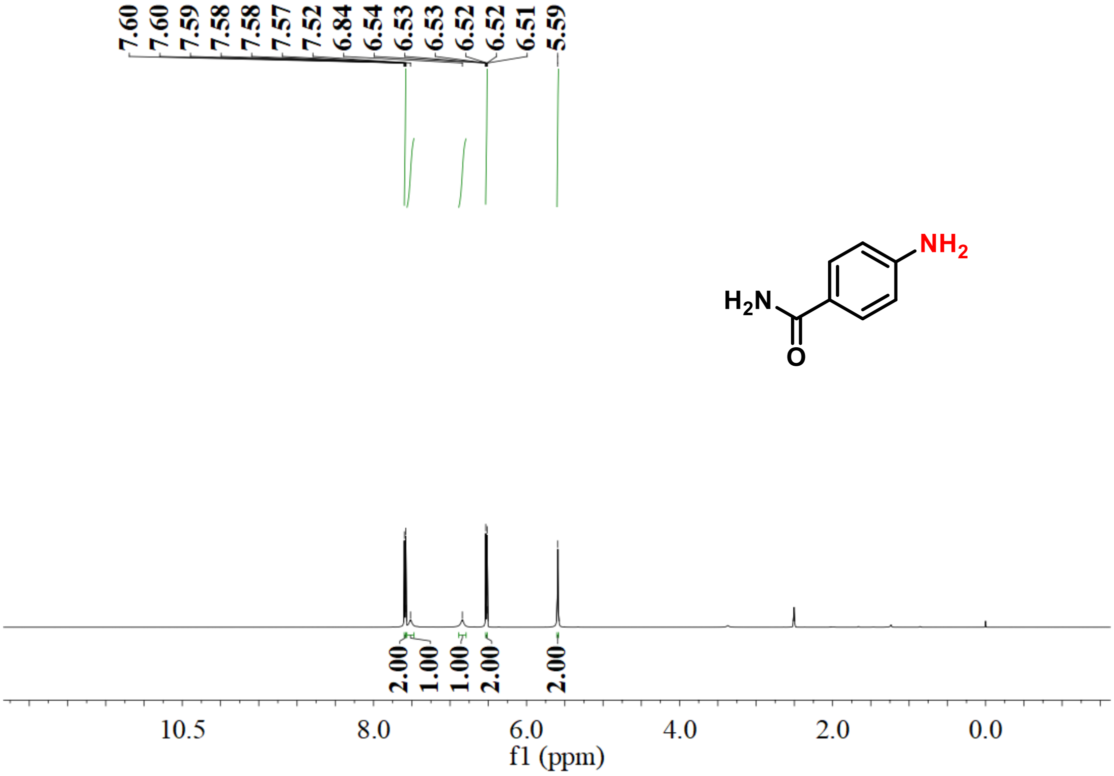

2o ^{13}C NMR

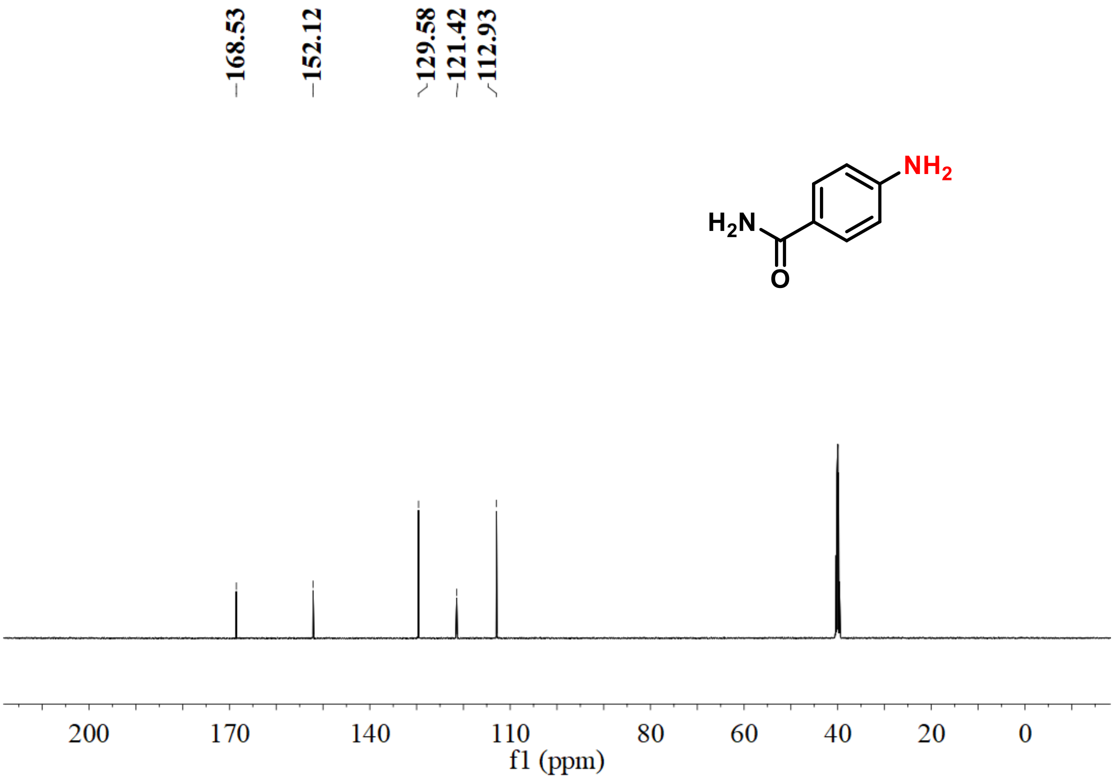

2p ^{1}H NMR

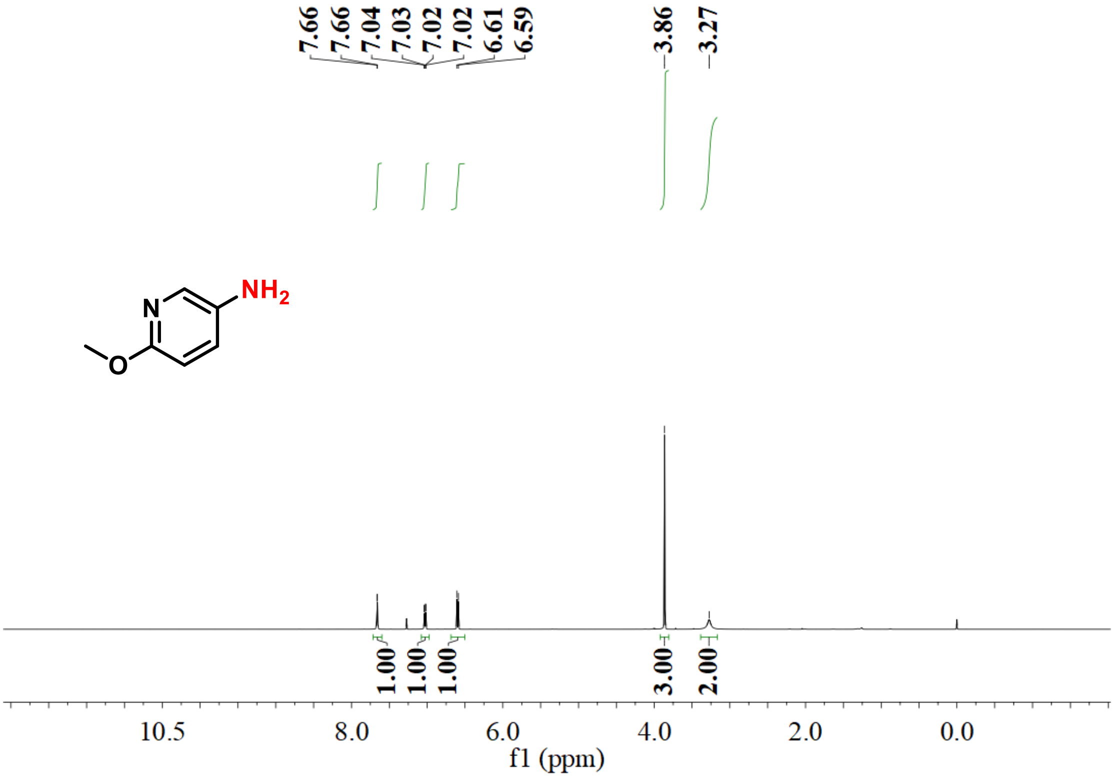

2p ^{13}C NMR

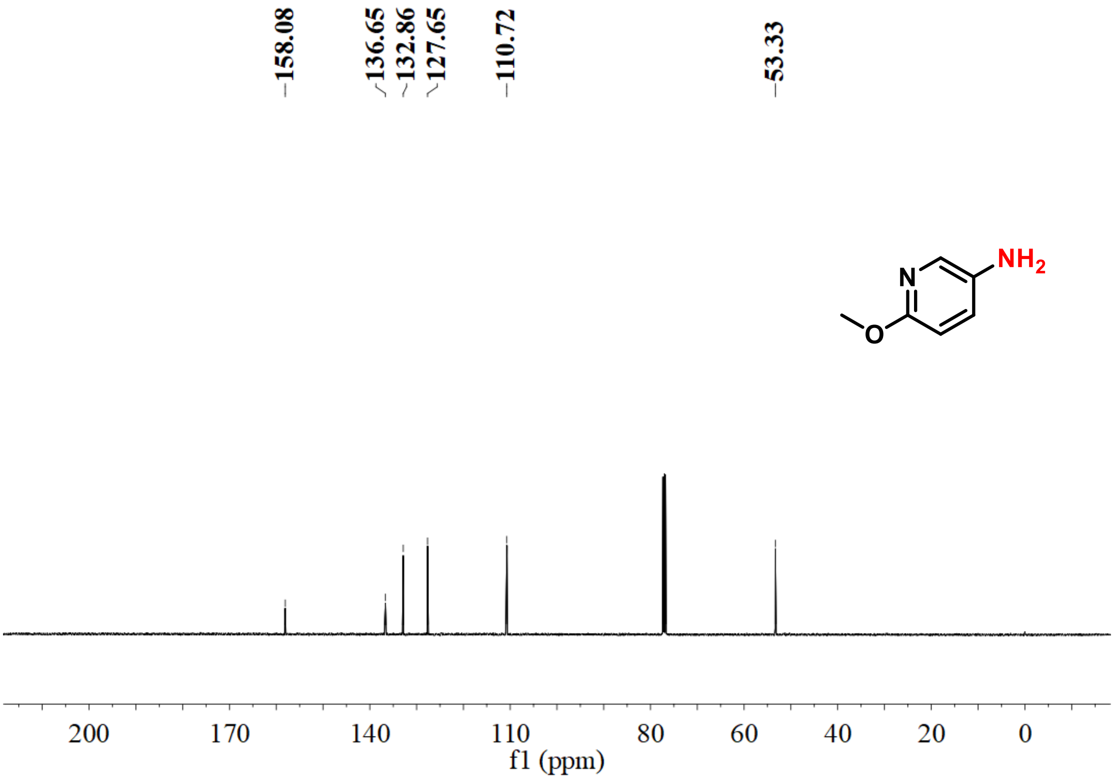

2q ¹H NMR

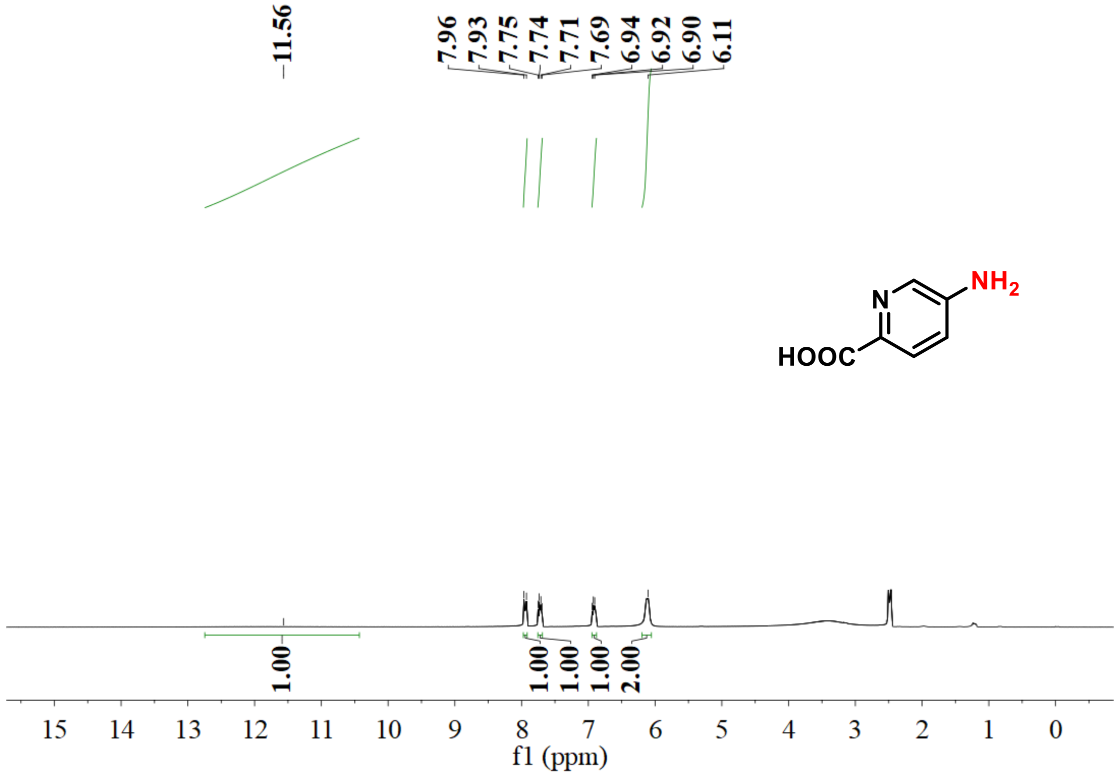

2q ¹³C NMR

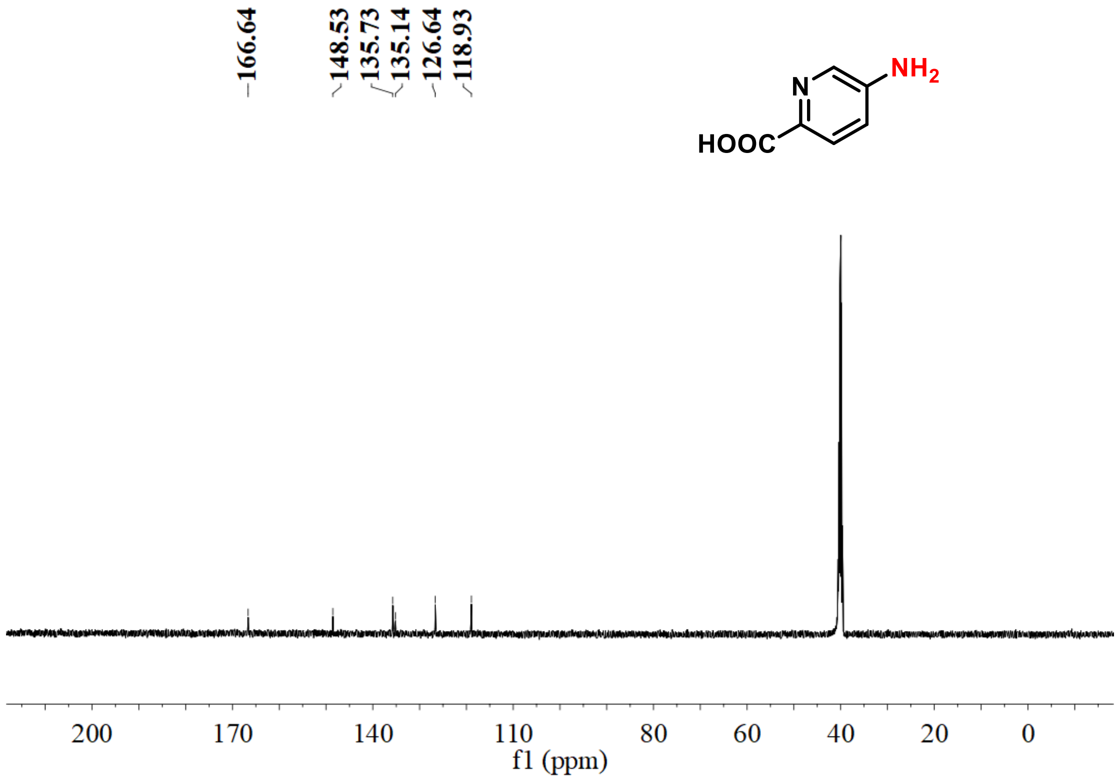

2a' ¹H NMR

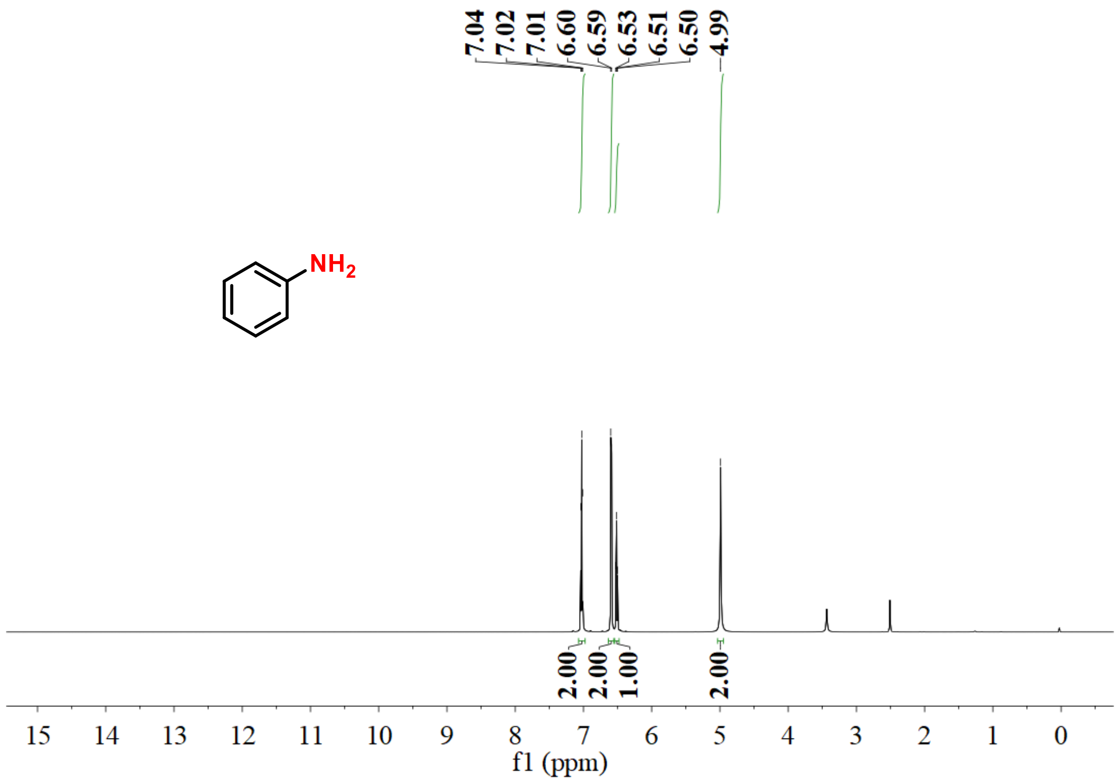

2a' ¹³C NMR

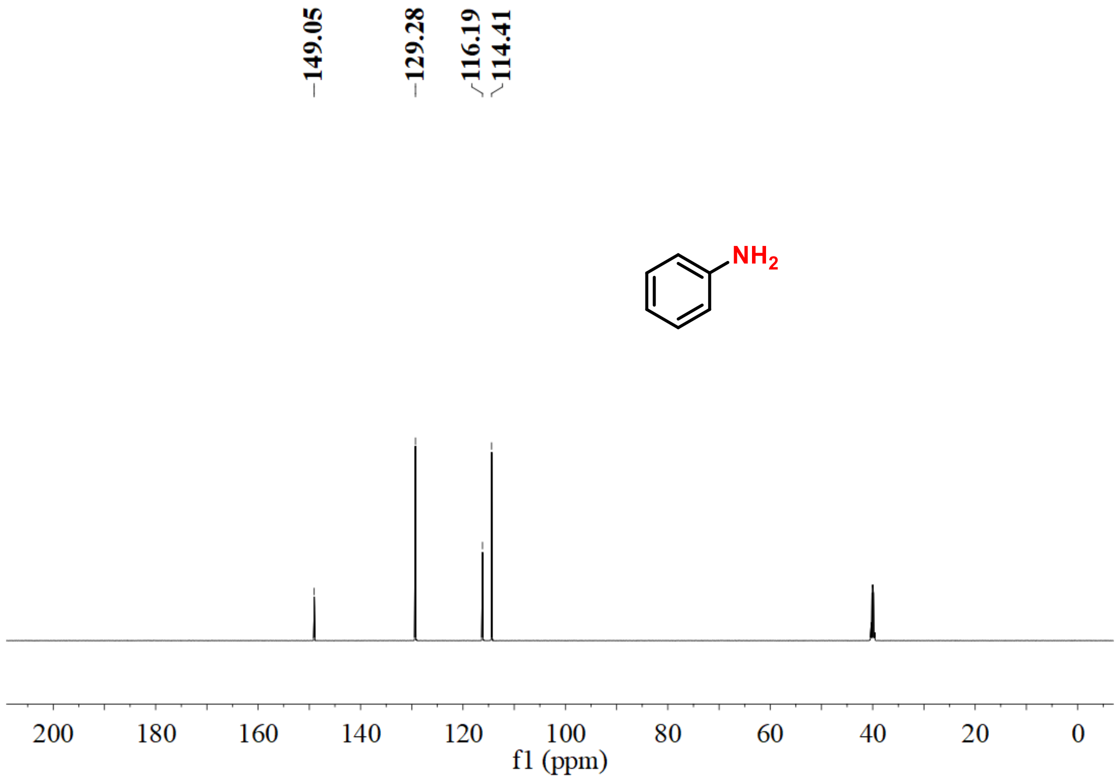

References

1. Yang, P.D.; Zhao, D.Y.; Chmelka, B.F.; Stucky, G.D. Triblock-copolymer-directed syntheses of large-pore mesoporous silica fibers. *Chem. Mater.* **1998**, *10*, 2033-2036, doi:DOI 10.1021/cm980201q.
2. Eli, L.D.; Kavuri, S.M.; Liu, Z.Y.; Su, J.; Xiao, Y.; Qiao, B.T.; Ding, Y.J. NiO_x-promoted Cu-based catalysts supported on AlSBA-15 for chemoselective hydrogenation of nitroarenes. *J. Catal.* **2022**, *416*, 332-343, doi:10.1016/j.jcat.2022.11.022.
3. Ding, S.M.; Cheng, D.; Xiao, W.M.; Ma, X.H.; Zeng, R.; Liu, S.Q.; Liang, S.Q.; Chen, C.; Song, W.G. Nickel Nanoparticles Encapsulated in Carbon Nanotubes as an Efficient and Robust Catalyst for Hydrogenation of Nitroarenes. *Catal. Lett.* **2023**, *153*, 595-604, doi:10.1007/s10562-022-04007-1.
4. Krishnan, S.; Patel, P.N.; Balasubramanian, K.K.; Chadha, A. Yeast supported gold nanoparticles: an efficient catalyst for the synthesis of commercially important aryl amines. *New J. Chem.* **2021**, *45*, 1915-1923, doi:10.1039/d0nj04542j.
5. Kara, B.Y.; Kilbas, B.; Goksu, H. Selectivity and activity in catalytic hydrogenation of azido groups over Pd nanoparticles on aluminum oxy-hydroxide. *New J. Chem.* **2016**, *40*, 9550-9555, doi:10.1039/c6nj01925k.
6. Huang, L.; Tang, F.Y.; Hao, F.; Zhao, H.; Liu, W.Y.; Lv, Y.; Liu, P.L.; Xiong, W.; Luo, H.A. Tuning the Electron Density of Metal Nickel via Interfacial Electron Transfer in Ni/MCM-41 for Efficient and Selective Catalytic Hydrogenation of Halogenated Nitroarenes. *ACS Sustainable Chem. Eng.* **2022**, *10*, 2947-2959, doi:10.1021/acssuschemeng.1c07836.
7. Zhang, R.K.; Chen, T.; Wang, G.S.; Guan, Y.Q.; Yan, G.Y.; Chen, Z.P.; Hu, J.S. Magnetic Recyclable Cu/$ZnFe_2O_4$ for Catalytic Reduction of Nitroarenes and C-N Bond Formation Reactions. *Catal. Lett.* **2022**, *152*, 3506-3516, doi:10.1007/s10562-021-03906-z.
8. Qu, Z.H.; Chen, X.; Zhong, S.; Deng, G.J.; Huang, H.W. NaI/PPh_3-Mediated Photochemical Reduction and Amination of Nitroarenes. *Org. Lett.* **2021**, *23*, 5349-5353, doi:10.1021/acs.orglett.1c01654.
9. Almeida, A.F.; Ataide, F.A.P.; Loureiro, R.M.S.; Moreira, R.; Rodrigues, T. Augmenting Adaptive Machine Learning with Kinetic Modeling for Reaction Optimization. *J. Org. Chem.* **2021**, *86*, 14192-14198, doi:10.1021/acs.joc.1c01038.
10. Zhang, Y.; Cheng, Y.J.; Wang, X.L.; Sun, Q.D.; He, X.H.; Ji, H.B. Enhanced Hydrogenation Properties of Pd Single Atom Catalysts with Atomically Dispersed Ba Sites as Electronic Promoters. *ACS Catal.* **2022**, doi:10.1021/acscatal.2c04626.
11. Guo, B.B.; de Vries, J.G.; Otten, E. Hydration of nitriles using a metal-ligand cooperative ruthenium pincer catalyst. *Chem. Sci.* **2019**, *10*, 10647-10652, doi:10.1039/c9sc04624k.
12. Quinn, J.F.; Bryant, C.E.; Golden, K.C.; Gregg, B.T. Rapid reduction of heteroaromatic nitro groups using catalytic transfer hydrogenation with microwave heating. *Tetrahedron Lett.* **2010**, *51*, 786-789, doi:10.1016/j.tetlet.2009.12.005.
13. Chang, J.B.; Hwang, J.H.; Park, J.S.; Kim, J.P. The effect of dye structure on the dyeing and optical properties of dichroic dyes for PVA polarizing film. *Dyes Pigm.* **2011**, *88*, 366-371, doi:10.1016/j.dyepig.2010.08.007.